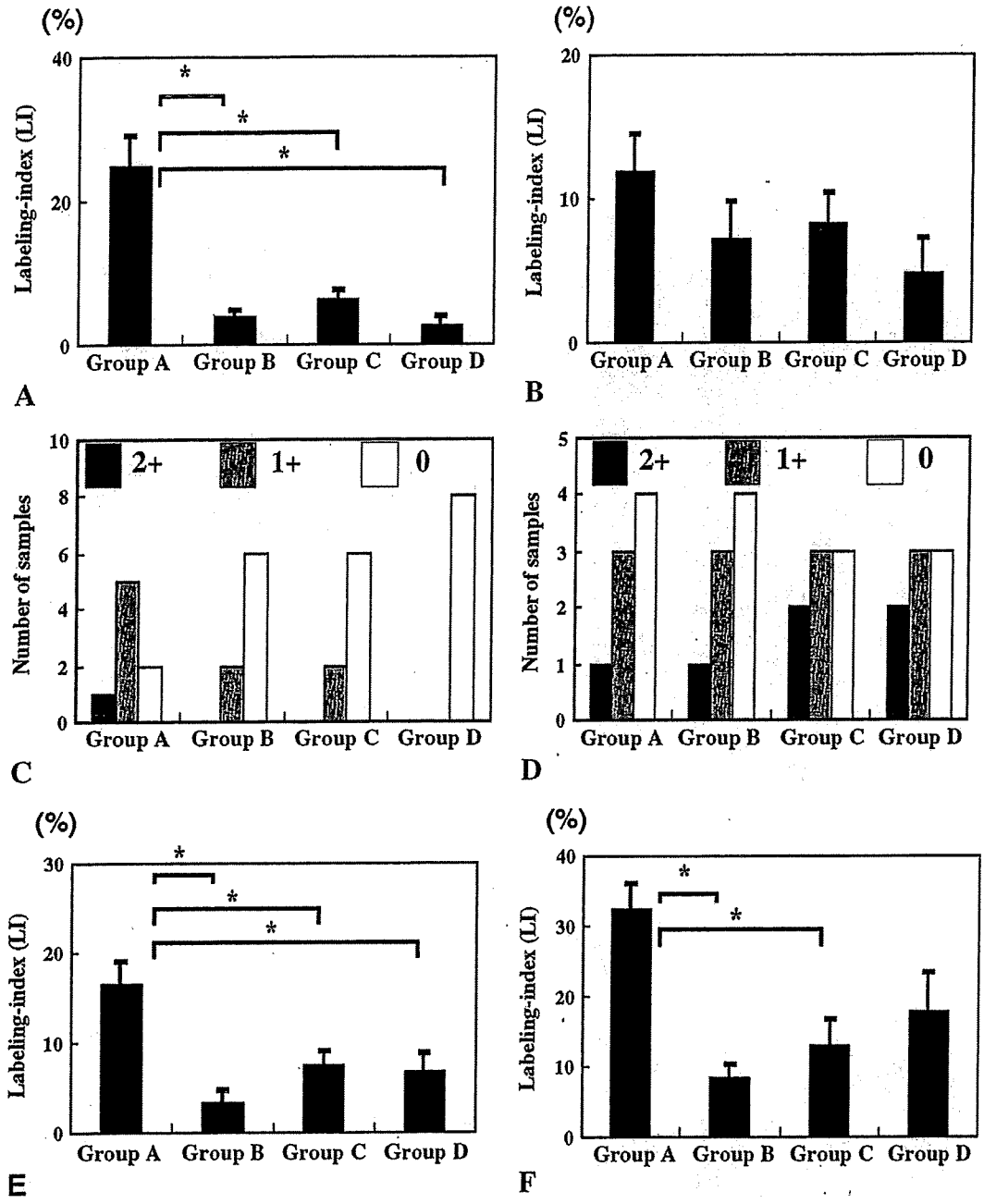

Figure 6. (A, B) The relative immunoreactivity of PTOV1 in the nuclei of VSMCs in the neointima (A) and media (B) was evaluated by the labelling index (LI) in each group (0–100), respectively. Data are the mean ± SEM. $^*p < 0.05$, a significant difference between two groups. (C, D) The relative immunoreactivity of PTOV1 in the cytoplasm of VSMCs in the neointima (C) and media (D) was evaluated by the percentage of positive cells (0, 1+, and 2+) in each group, respectively. (E, F) The relative immunoreactivity of AR present in the nuclei of VSMCs in the neointima (E) and media (F) was evaluated by the LI in each group (0–100), respectively. Data are the mean ± SEM. $^*p < 0.05$, a significant difference between two groups

have been reported as the mechanism for androgen-induced effects [19,20]. Therefore, further investigations are required to clarify how these pathways interact in exerting androgenic effects on VSMC proliferation in the human vascular system. Our present siRNA study demonstrated that *PTOV1* may be involved in testosterone-induced VSMC proliferation. However, further investigation is required to clarify the correlation between PTOV1 expression and testosterone-induced VSMC proliferation by reconstituting *PTOV1* expression after transfection of *PTOV1* siRNA.

Quantitative RT-PCR analysis in our present study also demonstrated that flutamide, an AR-blocker, suppressed androgen-induced *PTOV1* mRNA expression. The chromosomal region where *PTOV1* is located, 19q13.3–13.4, has also been demonstrated to harbour a large number of genes whose expression is modulated by androgens [14]. In addition, the expression of *PTOV1* was reported to be induced by exposure to androgens in LNCaP, an androgen-dependent prostate carcinoma cell line [14,17]. Therefore, these findings all indicate that *PTOV1* should also be considered one of the testosterone-induced genes in AR-positive VSMCs.

We also demonstrated that PTOV1 immunoreactivity in the nuclei of neointimal VSMCs was abundant in relatively young male aorta associated with early stage atherosclerosis. High levels and nuclear localization of PTOV1 have also been associated with cell proliferation in prostate carcinoma cells [14,17]. Neointimal VSMCs are, therefore, considered to play very important roles in the development of atherosclerosis in humans, particularly at an early stage, compared with VSMCs in the tunica media [10,11]. Therefore, higher expression of PTOV1 in these VSMCs is possibly related to the development of atherosclerosis. Levels of PTOV1 and AR were higher in male aorta with mild atherosclerosis than in female aorta with mild atherosclerosis. Men are generally considered to have a higher risk of developing cardiovascular disease than similarly aged women because of prolonged exposure to higher androgen concentrations [19,21]. It has also been shown recently that androgens upregulate atherosclerosis-related genes in macrophages from men, but not from women, which reflects the complexity of gender-related atherogenesis [19,22].

Our present study also demonstrated that the relative abundance of AR and PTOV1 in neointimal VSMCs was significantly higher in younger male aorta with mild atherosclerotic changes than in male aorta with severe atherosclerotic changes. However, these findings appear to contradict the hypothesis that, if PTOV1 is induced by androgens and implicated in androgenic effects on atherosclerosis, its expression should be higher in male aorta with more severe atherosclerosis than in male aorta with mild atherosclerosis owing to a longer exposure to elevated serum testosterone levels. There are two possible reasons for this: firstly, decreased AR and PTOV1 expression in the neointima of male aorta with severe atherosclerosis may be induced by the age-related decrease in serum testosterone levels [23]; and, secondly, when neointimal formation progresses, VSMCs with AR expression become less abundant than those without AR and these cells are therefore not necessarily influenced by androgenic atherogenic effects. Therefore, PTOV1 expression in the neointimal VSMCs in the aortas of men with high serum androgens levels may be associated with the androgen-induced onset of atherosclerosis; this may be important for formation of the neointima in the early stages of atherogenesis in the male aorta. However, recently, low concentrations of testosterone have been associated with an increased risk of cardiovascular disease in men [24]. Androgens are also known to be a coronary vasodilator, and a study of postmenopausal women demonstrated that endogenous androgens correlated inversely with carotid neointimal thickness, which suggests that androgens have potential beneficial effects on the human vascular system [19,25,26]. These different effects of androgens may depend on differences in the androgen-responsive genes induced, but further investigations are required to clarify possible direct androgenic effects on the human cardiovascular system.

In summary, *PTOV1* is considered to be one of the testosterone-induced genes involved in AR-mediated stimulation of VSMC proliferation in the aortic neointima and may play important roles in androgen-related atherogenesis in the male human aorta.

Acknowledgements

This work is in part supported by Health and Labour Sciences Research Grants for Risk Analysis Research on Food and Pharmaceuticals (H13-Seikatsu-013) from the Ministry of Health, Labour and Welfare of Japan. In addition, we thank Miss Naomi Kanai for technical assistance.

References

1. Wingard DL, Suarez L, Barrett-Connor E. The sex differential in mortality from all causes and ischemic heart disease. *Am J Epidemiol* 1983;**117:**165–172.
2. Lerner DJ, Kannel WM. Patterns of coronary heart disease morbidity and mortality in the sexes: a 26-year follow-up of the Framingham Study. *Am Heart J* 1986;**111:**383–390.
3. McCrohon JA, Jessup W, Handelsman DJ, Celermajer DS. Androgen exposure increases human monocyte adhesion to vascular endothelium and endothelial cell expression of vascular cell adhesion molecule-1. *Circulation* 1999;**99:**2317–2322.
4. McCrohon JA, Death AK, Nakhla S, Jessup W, Handelsman DJ, Stanley KK, *et al.* Androgen receptor expression is greater in macrophages from male than from female donors. A sex difference with implications for atherogenesis. *Circulation* 2000;**101:**224–226.
5. Jones RD, Hugh Jones T Channer KS. The influence of testosterone upon vascular reactivity. *Eur J Endocrinol* 2004;**151:**29–37.
6. Adams MR, Williams JK, Kaplan JR. Effects of androgens on coronary artery atherosclerosis and atherosclerosis-related impairment of vascular responsiveness. *Arterioscler Thromb Vasc Biol* 1995;**15:**562–570.
7. McCrohon JA, Jessup W, Handelsman DJ, Celermajer DS. Androgen exposure increases human monocyte adhesion to vascular endothelium and endothelial cell expression of vascular cell adhesion molecule-1. *Circulation* 1999;**99:**2317–2322.
8. Herman SM, Robinson JTC, McCredie RJ, Adams MR, Boyer MJ, Celermajer DS. Androgen deprivation is associated with enhanced endothelium-dependent dilatation in adult men. *Arterioscler Thromb Vasc Biol* 1997;**17:**2004–2009.
9. Liu PY, Death AK, Handelsman DJ. Androgens and cardiovascular disease. *Endocr Rev* 2003;**24:**313–340.
10. Nakamura Y, Igarashi K, Suzuki T, Kanno J, Inoue T, Tazawa C, *et al.* E4F1, a novel estrogen-responsive gene in possible atheroprotection, revealed by microarray analysis. *Am J Pathol* 2004;**165:**2019–2031.
11. Nakamura Y, Suzuki T, Miki Y, Tazawa C, Senzaki K, Moriya T, *et al.* Estrogen receptors in atherosclerotic human aorta: inhibition of human vascular smooth muscle cell proliferation by estrogens. *Mol Cell Endocrinol* 2004;**219:**17–26.
12. Kondo E, Horii A, Fukushige S. The human PMS2L proteins do not interact with hMLH1, a major DNA mismatch repair protein. *J Biochem (Tokyo)* 1999;**125:**818–825.
13. Jaffe IZ, Mendelsohn ME. Angiotensin II and Aldosterone regulate gene transcription via functional mineralocortocoid receptors in human coronary artery smooth muscle cells. *Circ Res* 2005;**96:**643–650.
14. Benedit P, Paciucci R, Thomson TM, Valeri M, Nadal M, Caceres C, *et al.* PTOV1, a novel protein overexpressed in prostate cancer containing a new class of protein homology blocks. *Oncogene* 2001;**20:**1455–1464.
15. Santamaria A, Castellanos E, Gomez V, Benedit P, Renau-Piqueras J, Morote J, *et al.* PTOV1 enables the nuclear

translocation and mitogenic activity of flotillin-1, a major protein of lipid rafts. *Mol Cell Biol* 2005;**25:**1900–1911.
16. Soslow RA, Dannenberg AJ, Rush D, Woerner BM, Khan KN, Masferrer J, *et al.* COX-2 is expressed in human pulmonary, colonic, and mammary tumors. *Cancer* 2000;**89:**2637–2645.
17. Santamaria A, Fernandez PL, Farre X, Benedit P, Reventos J, Morote J, *et al.* PTOV-1, a novel protein overexpressed in prostate cancer, shuttles between the cytoplasm and the nucleus and promotes entry into the S phase of the cell division cycle. *Am J Pathol* 2003;**162:**897–905.
18. Koike G, Winer ES, Horiuchi M, Brown DM, Szpirer C, Dzau VJ, *et al.* Cloning, characterization, and genetic mapping of the rat type 2 angiotensin II receptor gene. *Hypertension* 1995;**26:**998–1002.
19. Hashimura K, Sudhir K, Nigro J, Ling S, Williams MR, Komesaroff PA, *et al.* Androgens stimulate human vascular smooth muscle cell proteoglycan biosynthesis and increase lipoprotein binding. *Endocrinology* 2005;**146:**2085–2090.
20. Williams MR, Ling S, Dawood T, Hashimura K, Dai A, Li H, *et al.* Dehydroepiandrosterone inhibits human vascular smooth muscle cell proliferation independent of ARs and ERs. *J Clin Endocrinol Metab* 2002;**87:**176–181.
21. Gorodeski G, Utian W. Epidemiology and risk factors of cardiovascular disease in postmenopausal women. In *Treatment of the Postmenopausal Woman: Basic and Clinical Aspects*, Lobo R (ed). Raven Press: New York, 1994; 199–221.
22. Ng MK, Quinn CM, McCrohon JA, Nakhla S, Jessup W, Handelsman DJ, *et al.* Androgens up-regulate atherosclerosis-related genes in macrophages from males but not females: molecular insights into gender differences in atherosclerosis. *J Am Coll Cardiol* 2003;**42:**1306–1313.
23. Snyder PJ, Peachey H, Hannoush P, Berlin JA, Loh L, Lenrow DA, *et al.* Effect of testosterone treatment on body composition and muscle strength in men over 65 years of age. *J Clin Endocrinol Metab* 1999;**84:**2647–2653.
24. Fukui M, Kitagawa Y, Nakamura N, Kadono M, Mogami S, Hirata Ç, *et al.* Association between serum testosterone concentration and carotid atherosclerosis in men with type 2 diabetes. *Diabetes Care* 2003;**26:**1869–1873.
25. Chou TM, Sudhir K, Hutchison SJ, Ko E, Amidon TM, Collins P, *et al.* Testosterone induces dilation of canine coronary conductance and resistance arteries in vivo. *Circulation* 1996;**94:**2614–2619.
26. Bernini GP, Moretti A, Sgro M, Argenio GF, Barlascini CO, Cristofani R, *et al.* Influence of endogenous androgens on carotid wall in postmenopausal women. *Menopause* 2001;**8:**43–50.

Premature ovarian failure in androgen receptor-deficient mice

Hiroko Shiina*†‡, Takahiro Matsumoto*‡§, Takashi Sato*, Katsuhide Igarashi¶, Junko Miyamoto*, Sayuri Takemasa*, Matomo Sakari*§, Ichiro Takada*, Takashi Nakamura*§, Daniel Metzger‖, Pierre Chambon‖, Jun Kanno¶, Hiroyuki Yoshikawa†, and Shigeaki Kato*§**

*Institute of Molecular and Cellular Biosciences, University of Tokyo, 1-1-1 Yayoi, Bunkyo-ku, Tokyo 113-0032, Japan; §Exploratory Research for Advanced Technology, Japan Science and Technology, 4-1-8 Honcho, Kawaguchi, Saitama 332-0012, Japan; †Department of Obstetrics and Gynecology, Institute of Clinical Medicine, University of Tsukuba, 1-1-1 Tennoudai, Tsukuba, Ibaraki 305-8575, Japan; ¶Division of Cellular and Molecular Toxicology, National Institute of Health Sciences, 1-18-1 Kamiyoga, Setagaya-ku, Tokyo 158-8501, Japan; and ‖Institut de Genetique et de Biologie Moleculaire et Cellulaire, Centre National de la Recherche Scientifique, Institut National de la Santé et de la Recherche Médicale, Universite Louis Pasteur, College de France, 67404 Illkirch, Strasbourg, France

Edited by Bert W. O'Malley, Baylor College of Medicine, Houston, TX, and approved November 10, 2005 (received for review August 5, 2005)

Premature ovarian failure (POF) syndrome, an early decline of ovarian function in women, is frequently associated with X chromosome abnormalities ranging from various Xq deletions to complete loss of one of the X chromosomes. However, the genetic locus responsible for the POF remains unknown, and no candidate gene has been identified. Using the Cre/LoxP system, we have disrupted the mouse X chromosome androgen receptor (*Ar*) gene. Female $AR^{-/-}$ mice appeared normal but developed the POF phenotype with aberrant ovarian gene expression. Eight-week-old female $AR^{-/-}$ mice are fertile, but they have lower follicle numbers and impaired mammary development, and they produce only half of the normal number of pups per litter. Forty-week-old $AR^{-/-}$ mice are infertile because of complete loss of follicles. Genome-wide microarray analysis of mRNA from $AR^{-/-}$ ovaries revealed that a number of major regulators of folliculogenesis were under transcriptional control by AR. Our findings suggest that AR function is required for normal female reproduction, particularly folliculogenesis, and that AR is a potential therapeutic target in POF syndrome.

male hormone | nuclear receptor | female physiology | folliculogenesis | kit ligand

Premature ovarian failure (POF) is defined as an early decline of ovarian function after seemingly normal folliculogenesis (1). Genetic causes of POF have been frequently associated with X chromosome abnormalities (1, 2). Complete loss of one of the X chromosomes, as in Turner syndrome, and various Xq deletions are commonly identified as a cause of POF. However, responsible X-linked genes and their downstream targets have not been identified so far.

The androgen receptor (*Ar*) gene, which is the only sex hormone receptor gene on the X chromosome, is well known to be essential not only for the male reproductive system, but also for male physiology. In contrast, androgens are considered as male hormones; therefore, little is known about androgens' actions in female physiology, although AR expression in growing follicles has been described (3). However, because excessive androgen production in polycystic ovary syndrome causes infertility with abnormal menstrual cycles (4, 5), it is possible that AR-mediated androgen signaling also plays an important physiological role in the female reproductive system. Recently, using Cre/LoxP system, we generated an AR-null mutant mouse line (6) and demonstrated that inactivation of AR resulted in arrest of testicular development and spermatogenesis, impaired brain masculinization, high-turnover osteopenia, and late onset of obesity in males (7–9). At the same time, no overt physical or growth abnormalities were observed in female $AR^{-/-}$ mice. Therefore, to further examine potential role of AR in female physiology, we characterized female reproductive system in $AR^{-/-}$ females. Herein we show that female $AR^{-/-}$ mice develop the POF phenotype. At 3 weeks of age, $AR^{-/-}$ females had apparently normal ovaries with numbers of follicles similar to those in the wild-type females. However, thereafter the number of healthy follicles in the $AR^{-/-}$ ovary gradually declined, with a marked increase of atretic follicles, and by 40 weeks $AR^{-/-}$ mice became infertile, with no follicle detectable in the ovary. Reflecting this age-dependent progression in ovarian abnormality, several genes known to be involved in the oocyte–granulosa cell regulatory loop were identified by microarray analysis as AR downstream target genes. These findings clearly demonstrate that AR-mediated androgen signaling is indispensable for the maintenance of folliculogenesis and implicate impaired androgen signaling as a potential cause of the POF syndrome.

Materials and Methods

Generation of AR Knockout Mice. *AR* genomic clones were isolated from a TT2 embryonic stem cell genomic library by using human *AR* A/B domain cDNA as a probe (6). The targeting vector consisted of a 7.6-kb 5′ region containing exon 1, a 1.3-kb 3′ homologous region, a single loxP site, and a neo cassette with two loxP sites (10). Targeted clones (FB-18 and FC-61) were aggregated with single eight-cell embryos from CD-1 mice (11, 12). Floxed *AR* mice (C57BL/6) were then crossed with CMV-Cre transgenic mice (6). The two lines exhibited the same phenotypic abnormalities. The chromosomal sex of each pup was determined by genomic PCR amplification of the Y chromosome *Sry* gene (13).

Western Blot Analysis. To detect AR protein expression, ovarian cell lysates were separated by SDS/PAGE and transferred onto nitrocellulose membranes (14). Membranes were probed with polyclonal AR antibodies (N-20; Santa Cruz Biotechnology), and blots were visualized by using peroxidase-conjugated second antibody and an ECL detection kit (Amersham Pharmacia Biosciences).

Morphologic Classification of Growing Follicles. Sections were taken at intervals of 30 μm, and 6-μm paraffin-embedded sections were mounted on slides. Routine hematoxylin and eosin staining was performed for histologic examination by light microscopy. Follicle numbers in 12 sections per ovary were evaluated as primary follicles (oocyte surrounded by a single layer of cuboidal granulosa cells), preantral follicles (oocyte surrounded by two or

Conflict of interest statement: No conflicts declared.

This paper was submitted directly (Track II) to the PNAS office.

Abbreviations: AR, androgen receptor; DHT, 5α-dihydrotestosterone; POF, premature ovarian failure.

†H.S. and T.M. contributed equally to this work.

**To whom correspondence should be addressed. E-mail: uskato@mail.ecc.u-tokyo.ac.jp.

www.pnas.org/cgi/doi/10.1073/pnas.0506736102

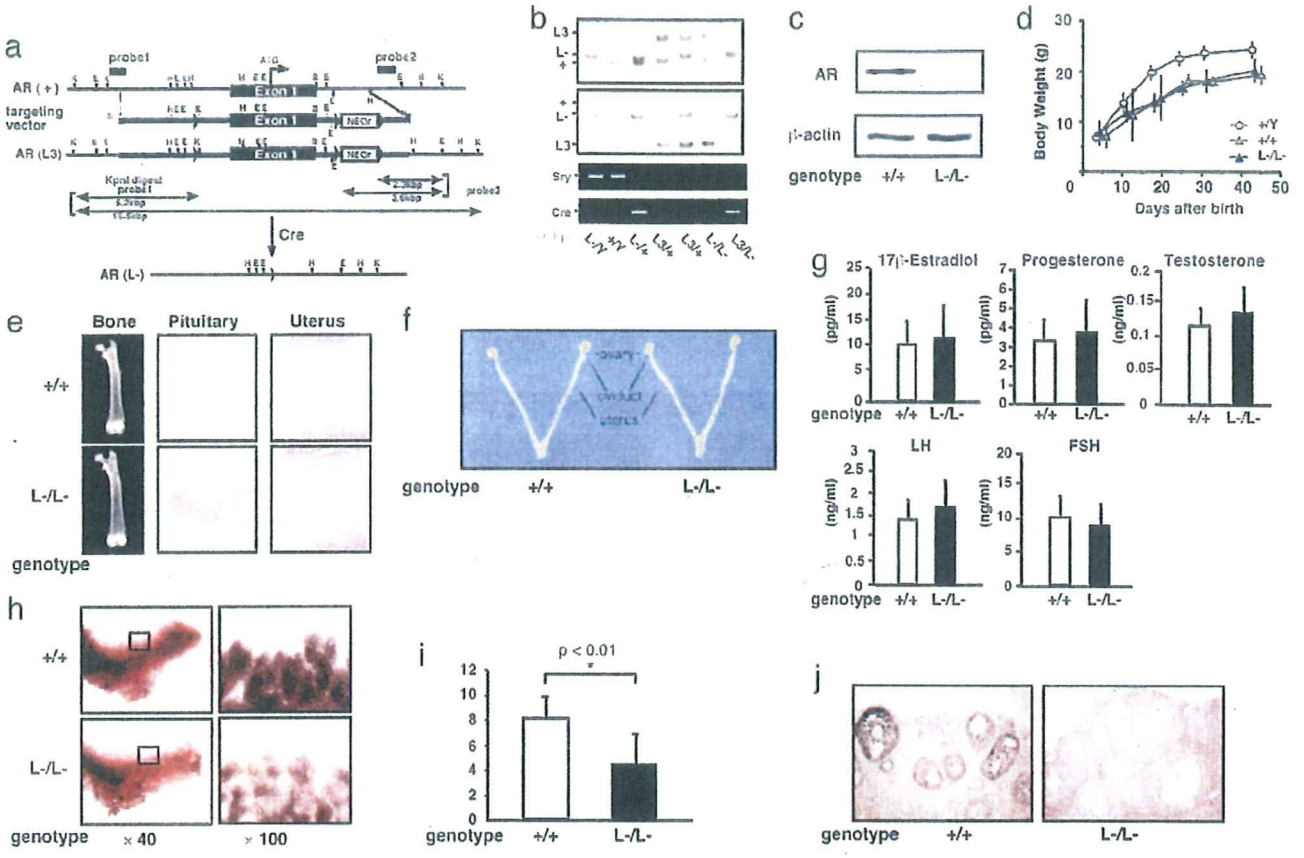

Fig. 1. Phenotypic characterization of AR knockout female mice. (*a*) Diagram of the wild-type *Ar* genomic locus (+), floxed *AR* L3 allele (L3), and *AR* allele (L-) obtained after Cre-mediated excision of exon 1. K, KpnI; E, EcoRI; H, HindIII; B, BamHI. LoxP sites are indicated by arrowheads. The targeting vector consisted of a 7.6-kb 5′ homologous region containing exon 1, a 1.3-kb 3′ homologous region, a single loxP site, and the neo cassette with two loxP sites. (*b*) Detection of the Y chromosome-specific *Sry* gene in $AR^{-/Y}$ mice by PCR. (*c*) Absence of AR protein in $AR^{-/-}$ mice ovaries by Western blot analysis using a specific C-terminal antibody. (*d*) Normal weight gain in $AR^{-/-}$ females. (*e*) Histology of pituitary, uterus, and bone tissues in $AR^{-/+}$ and $AR^{-/-}$ females at 8 weeks of age. (*f*) Female reproductive organs were macroscopically normal in $AR^{-/-}$ mice. (*g*) Serum hormone levels at the proestrus stage in $AR^{-/-}$ mice were not significantly altered. Serum 17β-estradiol, progesterone, testosterone, luteinizing hormone (LH), and follicle-stimulating hormone (FSH) levels in $AR^{+/+}$ ($n = 13$) and $AR^{-/-}$ ($n = 10$) females at 8–10 weeks of age are shown. (*h*) Lobuloalveolar development is impaired in $AR^{-/-}$ mammary glands. Whole mount of inguinal mammary glands (*Left*) and its higher magnification (*Right*) were prepared on day 3 of lactation. (*i*) Average number of pups per litter is markedly reduced in $AR^{-/-}$ mice at 8 weeks of age. Data are shown as mean ± SEM and analyzed by using Student's *t* test. (*j*) AR immunocytochemistry in $AR^{+/-}$ and $AR^{-/-}$ ovaries. Sections were counterstained with eosin.

more layers of granulosa cells with no antrum), or antral follicles (antrum within the granulosa cell layers enclosing the oocyte). Follicles were determined to be atretic if they displayed two or more of the following criteria within a single cross section: more than two pyknotic nuclei, granulosa cells within the antral cavity, granulosa cells pulling away from the basement membrane, or uneven granulosa cell layers (15).

Immunohistochemistry. Sections were subjected to a microwave antigen retrieval technique by boiling in 10 mM citrate buffer (pH 6.0) in a microwave oven for 30 min (16). The cooled sections were incubated in 1% H_2O_2 for 30 min to quench endogenous peroxidase and then incubated with 1% Triton X-100 in PBS for 10 min. To block nonspecific antibody binding, sections were incubated in normal goat serum for 1 h at 4°C. Sections were then incubated with anti-AR (1:100) or anti-cleaved caspase-3 (1:100) in 3% BSA overnight at 4°C. Negative controls were incubated in 3% BSA without primary antibody. The ABC method was used to visualize signals according to the manufacturer's instructions. Sections were incubated in biotinylated goat anti-rabbit IgG (1:200 dilution) for 2 h at room temperature, washed with PBS, and incubated in avidin–biotin–horseradish peroxidase for 1 h. After thorough washing in PBS, sections were developed with 3,3′-diaminobendizine tetrahydrochloride substrate, slightly counterstained with eosin, dehydrated through an ethanol series and xylene, and mounted.

Estrus Cycles and Fertility Test. To determine the stage of the estrus cycle (proestrus, estrus, and diestrus), vaginal smears were taken every morning and stained with Giemsa solution. For evaluation of female fertility for 15 weeks, an 8- or 24-week-old wild-type or $AR^{-/-}$ female was mated with a wild-type fertile male, replaced every 2 weeks with the other fertile male. Cages were monitored daily and for an additional 23 days, and the presence of seminal plugs and number of litters were recorded.

RNA Extraction and Quantitative Competitive RT-PCR. Total ovarian RNA was extracted by using TRIzol (Invitrogen) (16). Oligo-dT-primed cDNA was synthesized from 1 μg of ovarian RNA by using SuperScript reverse transcriptase (Gibco BRL, Gaithersburg, MD) in a 20-μl reaction volume, 1 μl of which was then diluted serially (2- to 128-fold) and used to PCR-amplify an internal control gene, *cycA*, to allow concentration estimation.

PHYSIOLOGY

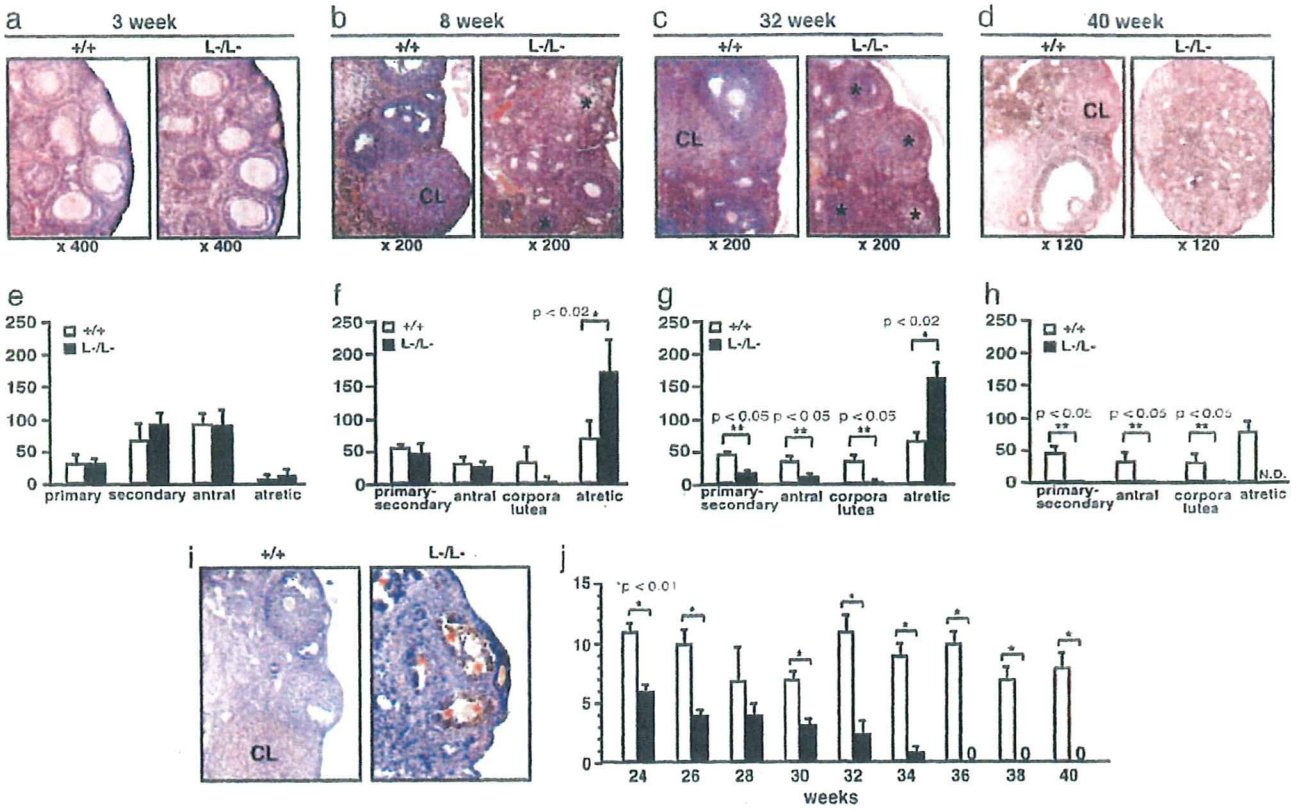

Fig. 2. POF in $AR^{-/-}$ female mice. (*a–d*) Histology of $AR^{+/+}$ and $AR^{-/-}$ ovaries at 3 weeks, 8 weeks, 32 weeks, and 40 weeks of age. All sections were stained with hematoxylin and eosin. An asterisk marks the atretic follicle. CL, corpus luteum. (*e–h*) Relative follicle counts at 3 weeks (*e*), 8 weeks (*f*), 32 weeks (*g*), and 40 weeks (*h*) of age. Numbers represent total counts of every fifth section from serially sectioned ovaries ($n = 4$ animals per genotype). (*i*) Immunohistochemical study for activated, cleaved caspase-3 revealed increased positive cells (apoptotic cells) in $AR^{-/-}$ ovaries. Sections were counterstained with hematoxylin. An asterisk marks the caspase-3-positive cell. CL, corpus luteum. (*j*) Age-dependent reduction in the number of pups per litter in $AR^{-/-}$ female mice. A continuous breeding assay was started at 24 weeks of age ($n = 6–10$ animals per genotype). For all panels, data are shown as mean ± SEM and were analyzed by using Student's *t* test.

Primers were designed from cDNA sequences of *Kitl* (M57647; nucleotides 1099–1751), Gdf9 (NM008110; nucleotides 720-1532), *Bmp15* (NM009757; nucleotides 146–973), *Ers2* (NM010157; nucleotides 1139–1921), *Pgr* (NM008829; nucleotides 1587–2425), *Cyp11a1* (NM019779; nucleotides 761-1697), *Cyp17al* (M64863; nucleotides 522–932), *Cyp19* (D00659; nucleotides 699-1049), *Fshr* (AF095642; nucleotides 625-1427), *Lhr* (M81310; nucleotides 592-1331), *Ptgs2* (AF338730; nucleotides 3–605), and *Ccnd2* (NM009829; nucleotides 150-1065) and chosen from different exons to avoid amplification from genomic DNA.

GeneChip Analysis. Ovaries were isolated and stabilized in RNA-*later* RNA Stabilization Reagent (Ambion, Austin, TX) before RNA purification (17). Total RNA was purified by using an RNeasy mini kit (Qiagen, Valencia, CA) according to the manufacturer's instructions. First-strand cDNA was synthesized from 5 μg of RNA by using 200 units of SuperScript II reverse transcriptase (Invitrogen, Carlsbad, CA), 100 pmol T7-$(dT)_{24}$ primer [5′-GGCCAGTGAATTGTAATACGACTCAC-TATAGGGAGGCGG-$(dT)_{24}$-3′], 1× first-strand buffer, and 0.5 mM dNTPs at 42°C for 1 h. Second-strand synthesis was performed by incubating first-strand cDNA with 10 units of *Escherichia coli* ligase (Invitrogen), 40 units of DNA polymerase I (Invitrogen), 2 units of RNase H (Invitrogen), 1× reaction buffer, and 0.2 mM dNTPs at 16°C for 2 h, followed by 10 units of T4 DNA polymerase (Invitrogen) and incubation for another 5 min at 16°C. Double-stranded cDNA was purified by using GeneChip Sample Cleanup Module (Affymetrix, Santa Clara, CA) according to the manufacturer's instructions and labeled by *in vitro* transcription by using a BioArray HighYield RNA transcript labeling kit (Enzo Diagnostics, Farmingdale, NY). Briefly, dsDNA was mixed with 1× HY reaction buffer, 1× biotin-labeled ribonucleotides (NTPs with Bio-UTP and Bio-CTP), 1× DTT, 1× RNase inhibitor mix, and 1× T7 RNA polymerase and incubated at 37°C for 4 h. Labeled cRNA was then purified by using GeneChip Sample Cleanup Module and fragmented in 1× fragmentation buffer at 94°C for 35 min. For hybridization to the GeneChip Mouse Expression Array 430A or 430B or Mouse Genome 430 2.0 Array (Affymetrix), 15 μg of fragmented cRNA probe was incubated with 50 pM control oligonucleotide B2, 1× eukaryotic hybridization control, 0.1 mg/ml herring sperm DNA, 0.5 mg/ml acetylated BSA, and 1× hybridization buffer in a 45°C rotisserie oven for 16 h. Washing and staining were performed by using a GeneChip Fluidic Station (Affymetrix) according to the manufacturer's protocol. Phycoerythrin-stained arrays were scanned as digital image files and analyzed with GENECHIP OPERATING SOFTWARE (Affymetrix) (17).

Luciferase Assay. The *Kitl* promoter region (−2866 to −1 bp) was inserted into the pGL3-basic vector (Promega) for assay using the Luciferase Assay System (Promega) (14, 16). Cells at 40–50% confluence were transfected with a reference pRL-CMV

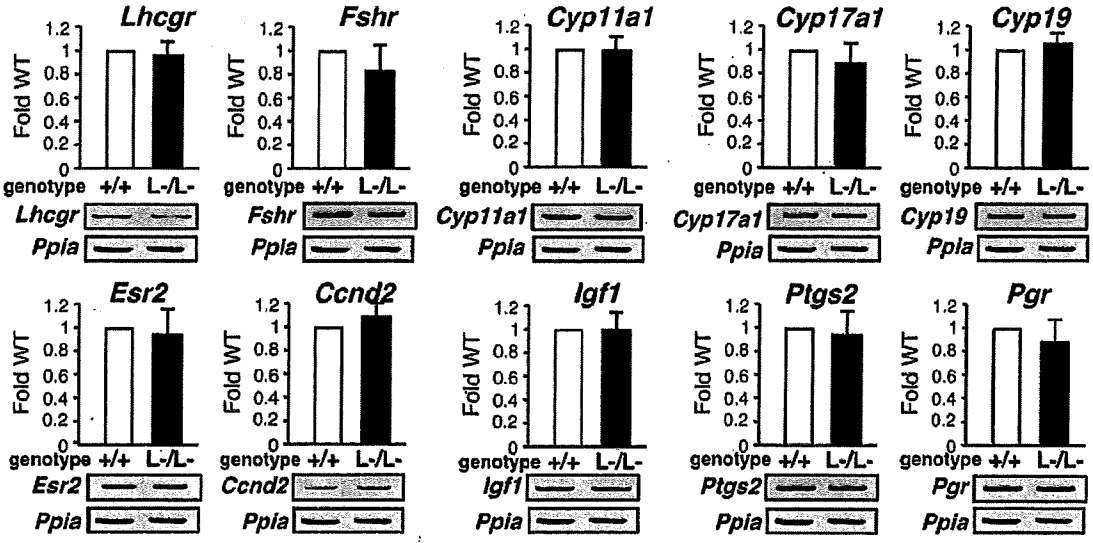

Fig. 3. No significant alterations in mRNA levels of several major regulators in folliculogenesis. Shown is semiquantitative RT-PCR of LH receptor (*Lhr*), FSH receptor (*Fshr*), p450 side chain cleavage enzyme (*Cyp11a1*), 17-α-hydroxylase (*Cyp17a1*), Aromatase (*Cyp19*), estrogen receptor-β (*Esr2*), cyclin D2 (*Ccnd2*), insulin-like growth factor 1 (*Igf1*), cyclooxygenase 2 (*Ptgs2*), or progesterone receptor (*Pgr*) gene expression in $AR^{+/+}$ and $AR^{-/-}$ ovaries. Results shown were representative (using one ovary per genotype in each experiment) of five independent experiments.

plasmid (Promega) using Lipofectamine reagent (GIBCO/BRL, Grand Island, NY) to normalize transfection. Results shown are representative of five independent experiments.

Results and Discussion

Subfertility of $AR^{-/-}$ Female Mice at 8 Weeks of Age. The *Ar* gene located on the X chromosome was disrupted in mice by using the Cre/Lox P system (6) (Fig. 1 *a–c*). Female $AR^{-/-}$ mice showed normal growth compared with the wild-type littermates (Fig. 1*d*), with no detectable bone loss (Fig. 1*e*) or obesity common for male $AR^{-/Y}$ mice (8, 9). Young (8-week-old) $AR^{-/-}$ females appeared indistinguishable from the wild-type littermates, displayed normal sexual behavior (7), and produced the first offspring of normal body size at the expected age. Macroscopic appearance of their reproductive organs, including uteri, oviducts, and ovaries, also appeared normal (Fig. 1*f*). Histological analysis showed no significant abnormality in the uterus or pituitary (Fig. 1*e*), whereas mammary ductal branching and elongation were substantially reduced, as revealed by whole-mount analysis (Fig. 1*h*). Serum levels of 17β-estradiol, progesterone, testosterone, luteinizing hormone, and follicle-stimulating hormone were also within normal range in 8-week-old mutant females at the proestrus stage (Fig. 1*g*), suggesting that the two-cell two-gonadotrophin system in female reproductive and endocrine organs (18) was intact in $AR^{-/-}$ mice at 8 weeks of age. The most obvious early sign of abnormal reproductive function in the $AR^{-/-}$ females was that their average numbers of pups per litter were only about half of those of the wild-type littermates, ($AR^{+/+}$, 8.3 ± 0.4 pups per litter; $AR^{-/-}$, 4.5 ± 0.5 pups per litter) (Fig. 1*i*).

$AR^{-/-}$ Female Mice Developed POF Phenotypes. Histological analysis of 8-week-old $AR^{-/-}$ ovaries clearly showed that numbers of atretic follicles were significantly increased, with decreased numbers of corpora lutea (Fig. 2 *b* and *f*). This finding suggests that the reduced pup numbers were due to impaired folliculogenesis in AR-deficient ovaries. Indeed, AR protein expression was readily detectable in the wild-type 8-week-old ovaries (Fig. 1*j*), with AR expressed at the highest levels in growing follicle granulosa cells at all developmental stages and at relatively low levels in corpora lutea. Thus, AR appears to play a regulatory role in granulosa cells during their maturation to the luteal phase.

To investigate this possibility, we examined the ovarian phenotype of female $AR^{-/-}$ mice at different ages. At 3 weeks, ovaries contain various stages of follicles, including primary, secondary, and antral follicles in wild-type animals (Fig. 2*a*) (19). In $AR^{-/-}$ ovaries at 3 weeks of age, the folliculogenesis appeared to be unaltered, with normal numbers and localization of primary and secondary follicles (Fig. 2 *a* and *e*). However, degenerated folliculogenesis became evident with further aging. Although follicles and corpora lutea at all developmental stages were still present, corpora lutea numbers were clearly reduced in 8-week-old $AR^{-/-}$ mutants (Fig. 2 *b* and *f*), similar to that observed in another mouse line (20). Expected apoptosis was seen in atretic follicles by activated caspase-3 immunohistochemistry assays (Fig. 2*i*). But, by 32 weeks of age, defects in folliculogenesis in $AR^{-/-}$ ovaries became profound, with fewer follicles observed and increased atretic follicles (Fig. 2 *c* and *g*), and >40% (5 of 12 mice) of the $AR^{-/-}$ females were already infertile. By 40 weeks, all $AR^{-/-}$ females became infertile, with no follicles remaining (Fig. 2 *d* and *h*); at the same age, $AR^{+/+}$ females were fertile and had normal follicle numbers. Consistent with progressive deficiency in folliculogenesis, the pup number per litter steadily decreased in aging $AR^{-/-}$ females (Fig. 2*i*). These data indicate that AR plays an important physiological role at the preluteal phase of folliculogenesis.

Alteration in Gene Expressions of Several Major Regulators Involved in the Oocyte–Granulosa Cell Regulatory Loop. To explore the molecular basis underlying the impaired folliculogenesis in $AR^{-/-}$ ovaries, we analyzed expression of several major known regulators and markers of folliculogenesis (21–23). Surprisingly, no significant alterations in mRNA levels of LH receptor (*Lhr*), FSH receptor (*Fshr*), p450 side chain cleavage enzyme (*Cyp11a1*), 17-α-hydroxylase (*Cyp17a1*), aromatase (*Cyp19*), estrogen receptor-β (*Esr2*), cyclin D2 (*Ccnd2*), or insulin-like growth factor 1 (*Igf1*) of 8-week-old $AR^{-/-}$ ovaries at the proestrus stage, and further cyclooxygenase 2 (*Ptgs2*) or progesterone receptor (*Pgr*) at the estrus stage, were detected by

PHYSIOLOGY

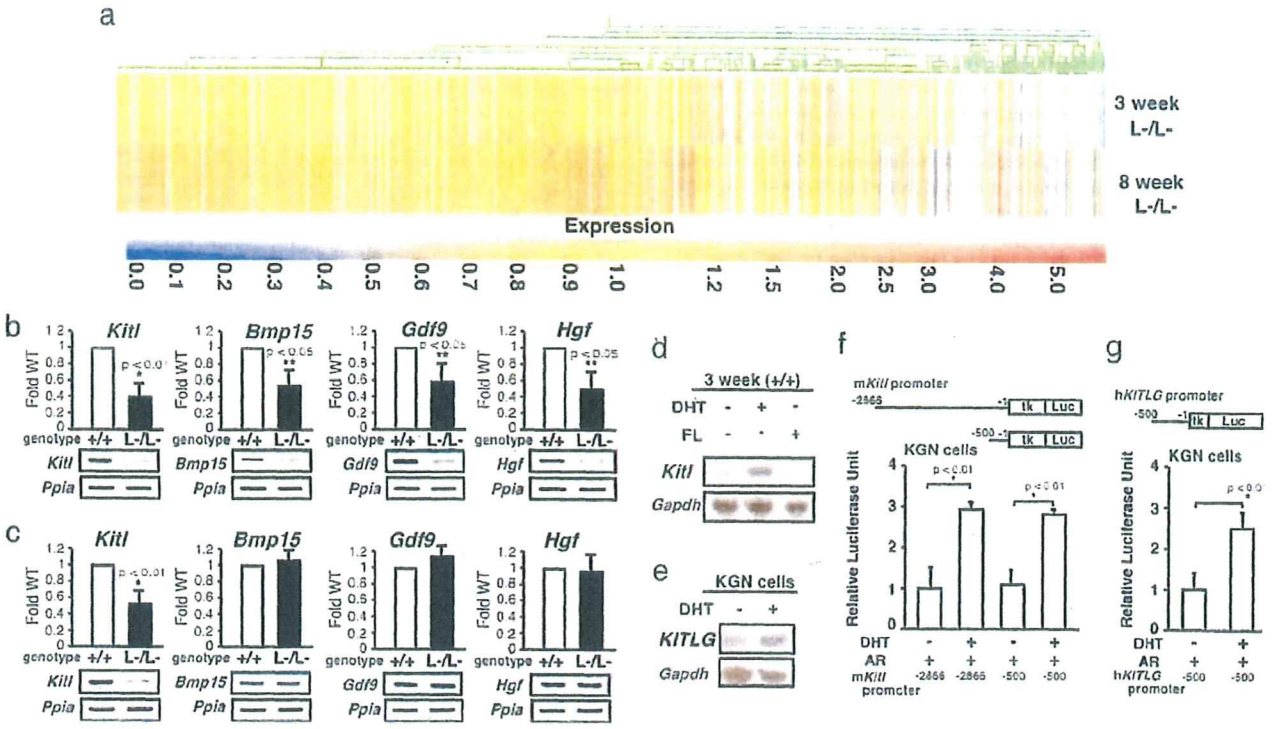

Fig. 4. Genome-wide microarray analysis and semiquantitative RT-PCR revealed that expression of the oocyte–granulosa cell regulator loop was down-regulated in $AR^{-/-}$ ovaries. (*a*) Microarray analysis of $AR^{-/-}$ compared with $AR^{+/+}$ ovaries at 3 and 8 weeks of age. Data obtained from microarray analysis as described in *Materials and Methods* were used to generate a cluster analysis. Each vertical line represents a single gene. The ratios of gene expression levels in $AR^{-/-}$ ovaries compared with wild type are presented. (*b* and *c*) Semiquantitative RT-PCR analysis of AR-regulated genes identified from the microarray study. Results shown are representative (using one ovary per genotype in each experiment) of five independent experiments. Data are shown as mean ± SEM and were analyzed by using Student's *t* test. (*d*) Comparison of *Kitl* gene expression by Northern blot analysis among placebo-, DHT-, and flutamide (FL)-treated $AR^{+/+}$ mouse ovaries. (*e*) Induction of *KITLG* gene expression by DHT treatment in KGN cells. (*f* and *g*) Androgen responsiveness in the mouse and human *kit ligand* promoters by a luciferase assay performed by using KGN cells. Data are shown as mean ± SEM and were analyzed by using Student's *t* test.

semiquantitative RT-PCR analysis (Fig. 3). Genome-wide microarray analysis (17) of RNA from 8-week-old $AR^{-/-}$ ovaries at the proestrus stage has been undertaken to identify AR-regulated genes. In comparison with $AR^{+/+}$ ovaries, expressions of 772 genes were down-regulated, whereas 351 genes were up-regulated in $AR^{-/-}$ ovaries (Fig. 4*a*; see also Tables 1 and 2, which are published as supporting information on the PNAS web site). Several genes known to be involved in the oocyte–granulosa cell regulatory loop (24) were identified as candidate AR target genes, including KIT ligand (*Kitl*) (25), morphogenetic protein 15 (*Bmp15*) (26), growth differentiation factor-9 (*Gdf9*) (27), and hepatocyte growth factor (*Hgf*) (28). Impaired folliculogenesis had been reported in mice deficient in each of these three regulators (26, 27, 29). To validate the microarray data, we performed semiquantitative RT-PCR analysis of 8-week-old $AR^{-/-}$ ovary RNA and confirmed that expression of these factors was down-regulated (Fig. 4*b*). To identify a regulator downstream of the AR signaling at an earlier stage of folliculogenesis, 3-week-old $AR^{-/-}$ ovaries that, as pointed out earlier, display no apparent phenotypic abnormality were examined. Fewer genes had altered expression levels (519 genes up-regulated; 326 genes down-regulated) (Fig. 4*a*; see also Tables 3 and 4, which are published as supporting information on the PNAS web site), and, of the four regulators tested by RT-PCR, only *Kitl* was found to be down-regulated at this age (Fig. 4*c*). Because *Kitl* is a granulosa cell-derived factor and stimulates oocyte growth and maturation (29–31), down-regulation of the *Kitl* expression in 3-week-old or even younger $AR^{-/-}$ ovaries may trigger impairment in folliculogenesis at a later age. To test for possible *Kitl* gene regulation by AR, 3-week-old wild-type females were treated with 5α-dihydrotestosterone (DHT). At 4 h after hormone injection, a clear induction of *Kitl* expression was observed in the ovaries, whereas a known antiandrogen flutamide attenuated the induction by DHT (Fig. 4*d*). The induction of endogenous human *kit ligand* (*KITLG*) gene by DHT was also observed in human granulosa-like tumor cells (KGN) in culture (Fig. 4*e*). Furthermore, androgen-induced transactivation of mouse and human *kit ligand* promoters (32) was observed by a luciferase reporter assay (33) in KGN (Fig. 4 *f* and *g*), 293T, and HeLa (data not shown) cells. However, no response to DHT was detected in the similar assay using promoters of the *Bmp15*, *Gdf9*, and *Hgf* genes (data not shown). Thus, we have shown that, in a regulatory cascade controlling folliculogenesis, *Kitl* represents a direct downstream target of androgen signaling.

As an upstream regulator, AR may also be indirectly involved in control of expression of other genes critical for folliculogenesis, because an age-dependent down-regulation of *Bmp15*, *Gdf9*, and *Hgf* gene expression was also observed in $AR^{-/-}$ ovaries. *Bmp15* and *Gdf9* are oocyte-derived factors that promote the development of surrounding granulosa cells in growing follicles (34, 35), whereas *Hgf* is secreted by theca cells and acts as a granulosa cell growth factor (36). Down-regulation of these factors, presumably due to decreased *Kitl* expression, may lead to impaired bidirectional communication between oocyte and granulosa cells (24) and, eventually, to early termination of folliculogenesis, as in POF syndrome.

Thus, we have identified AR as a novel regulator of follicu-

logenesis that apparently acts in the regulatory cascade upstream of the major factors controlling ovarian function, confirming the previous findings of the AR expression in granulose cells of growing follicles (3). Although not immediately relevant to the ovarian physiology, abnormal development of the mammary glands observed in our AR-deficient mice adds further strong evidence of an essential role of the AR not only in male, but also in female, reproductive function.

With increasing age of the first childbirth by women in the modern society, POF syndrome has become an important social and medical problem. Our findings suggest that POF syndrome may be caused by an impairment in androgen signaling and that X chromosomal mutations affecting the *AR* gene function may play a key role in hereditary POF. From clinical perspective, the present study provides evidence that AR can be a beneficial therapeutic target in treatment of POF syndrome patients.

We thank T. Iwamori and H. Tojo for expert advice on mammary gland anatomy, Y. Kanai for ovarian phenotypic analysis, members of the KO project team at the laboratory of Nuclear Signaling (Institute of Molecular and Cellular Biosciences) for their support, A. P. Kouzmenko for helpful suggestions, and H. Higuchi for manuscript preparation. This work was supported in part by the Program for Promotion of Basic Research Activities for Innovative Biosciences and priority areas from the Ministry of Education, Culture, Sports, Science, and Technology (to S.K.).

1. Laml, T., Preyer, O., Umek, W., Hengstschlager, M. & Hanzal, H. (2002) *Hum. Reprod. Update* **8**, 483–491.
2. Davison, R. M., Davis, C. J. & Conway, G. S. (1999) *Clin. Endocrinol. (Oxford)* **51**, 673–679.
3. Tetsuka, M., Whitelaw, P. F., Bremner, W. J., Millar, M. R., Smyth, C. D. & Hillier, S. G. (1995) *J. Endocrinol.* **145**, 535–543.
4. Ehrmann, D. A., Barnes, R. B. & Rosenfield, R. L. (1995) *Endocr. Rev.* **16**, 322–353.
5. Norman, R. J. (2002) *Mol. Cell. Endocrinol.* **191**, 113–119.
6. Kato, S. (2002) *Clin. Pediatr. Endocrinol.* **11**, 1–7.
7. Sato, T., Matsumoto, T., Kawano, H., Watanabe, T., Uematsu, Y., Sekine, K., Fukuda, T., Aihara, K., Krust, A., Yamada, T., *et al.* (2004) *Proc. Natl. Acad. Sci. USA* **101**, 1673–1678.
8. Sato, T., Matsumoto, T., Yamada, T., Watanabe, T., Kawano, H. & Kato, S. (2003) *Biochem. Biophys. Res. Commun.* **300**, 167–171.
9. Kawano, H., Sato, T., Yamada, T., Matsumoto, T., Sekine, K., Watanabe, T., Nakamura, T., Fukuda, T., Yoshimura, K., Yoshizawa, T., *et al.* (2003) *Proc. Natl. Acad. Sci. USA* **100**, 9416–9421.
10. Li, M., Indra, A. K., Warot, X., Brocard, J., Messaddeq, N., Kato, S., Metzger, D. & Chambon, P. (2000) *Nature* **407**, 633–636.
11. Sekine, K., Ohuchi, H., Fujiwara, M., Yamasaki, M., Yoshizawa, T., Sato, T., Yagishita, N., Matsui, D., Koga, Y., Itoh, N. & Kato, S. (1999) *Nat. Genet.* **21**, 138–141.
12. Yoshizawa, T., Handa, Y., Uematsu, Y., Takeda, S., Sekine, K., Yoshihara, Y., Kawakami, T., Arioka, K., Sato, H., Uchiyama, Y., *et al.* (1997) *Nat. Genet.* **16**, 391–396.
13. Gubbay, J., Collignon, J., Koopman, P., Capel, B., Economou, A., Munsterberg, A., Vivian, N., Goodfellow, P. & Lovell-Badge, R. (1990) *Nature* **346**, 245–250.
14. Yanagisawa, J., Yanagi, Y., Masuhiro, Y., Suzawa, M., Watanabe, M., Kashiwagi, K., Toriyabe, T., Kawabata, M., Miyazono, K. & Kato, S. (1999) *Science* **283**, 1317–1321.
15. Britt, K. L., Drummond, A. E., Cox, V. A., Dyson, M., Wreford, N. G., Jones, M. E., Simpson, E. R. & Findlay, J. K. (2000) *Endocrinology* **141**, 2614–2623.
16. Ohtake, F., Takeyama, K., Matsumoto, T., Kitagawa, H., Yamamoto, Y., Nohara, K., Tohyama, C., Krust, A., Mimura, J., Chambon, P., *et al.* (2003) *Nature* **423**, 545–550.
17. Fujimoto, N., Igarashi, K., Kanno, J., Honda, H. & Inoue, T. (2004) *J. Steroid Biochem. Mol. Biol.* **91**, 121–129.
18. Couse, J. F. & Korach, K. S. (1999) *Endocr. Rev.* **20**, 358–417.
19. Elvin, J. A. & Matzuk, M. M. (1998) *Rev. Reprod.* **3**, 183–195.
20. Hu, Y. C., Wang, P. H., Yeh, S., Wang, R. S., Xie, C., Xu, Q., Zhou, X., Chao, H. T., Tsai, M. Y. & Chang, C. (2004) *Proc. Natl. Acad. Sci. USA* **101**, 11209–11214.
21. Elvin, J. A., Yan, C., Wang, P., Nishimori, K. & Matzuk, M. M. (1999) *Mol. Endocrinol.* **13**, 1018–1034.
22. Zhou, J., Kumar, T. R., Matzuk, M. M. & Bondy, C. (1997) *Mol. Endocrinol.* **11**, 1924–1933.
23. Burns, K. H., Yan, C., Kumar, T. R. & Matzuk, M. M. (2001) *Endocrinology* **142**, 2742–2751.
24. Matzuk, M. M., Burns, K. H., Viveiros, M. M. & Eppig, J. J. (2002) *Science* **296**, 2178–2180.
25. Joyce, I. M., Pendola, F. L., Wigglesworth, K. & Eppig, J. J. (1999) *Dev. Biol.* **214**, 342–353.
26. Yan, C., Wang, P., DeMayo, J., DeMayo, F. J., Elvin, J. A., Carino, C., Prasad, S. V., Skinner, S. S., Dunbar, B. S., Dube, J. L., *et al.* (2001) *Mol. Endocrinol.* **15**, 854–866.
27. Dong, J., Albertini, D. F., Nishimori, K., Kumar, T. R., Lu, N. & Matzuk, M. M. (1996) *Nature* **383**, 531–535.
28. Parrott, J. A., Vigne, J. L., Chu, B. Z. & Skinner, M. K. (1994) *Endocrinology* **135**, 569–575.
29. Driancourt, M. A., Reynaud, K., Cortvrindt, R. & Smitz, J. (2000) *Rev. Reprod.* **5**, 143–152.
30. Huang, E. J., Manova, K., Packer, A. I., Sanchez, S., Bachvarova, R. F. & Besmer, P. (1993) *Dev. Biol.* **157**, 100–109.
31. Packer, A. I., Hsu, Y. C., Besmer, P. & Bachvarova, R. F. (1994) *Dev. Biol.* **161**, 194–205.
32. Grimaldi, P., Capolunghi, F., Geremia, R. & Rossi, P. (2003) *Biol. Reprod.* **69**, 1979–1988.
33. Kitagawa, H., Fujiki, R., Yoshimura, K., Mezaki, Y., Uematsu, Y., Matsui, D., Ogawa, S., Unno, K., Okubo, M., Tokita, A., *et al.* (2003) *Cell* **113**, 905–917.
34. Otsuka, F. & Shimasaki, S. (2002) *Proc. Natl. Acad. Sci. USA* **99**, 8060–8065.
35. Joyce, I. M., Clark, A. T., Pendola, F. L. & Eppig, J. J. (2000) *Biol. Reprod.* **63**, 1669–1675.
36. Parrott, J. A. & Skinner, M. K. (1998) *Endocrinology* **139**, 2240–2245.

American Journal of Pathology, Vol. 165, No. 6, December 2004

Vascular Biology, Atherosclerosis and Endothelium Biology

E4F1, a Novel Estrogen-Responsive Gene in Possible Atheroprotection, Revealed by Microarray Analysis

Yasuhiro Nakamura,*† Katsuhide Igarashi,‡ Takashi Suzuki,* Jun Kanno,‡ Tohru Inoue,§ Chika Tazawa,* Masayuki Saruta,* Tomoko Ando,‡ Noriko Moriyama,‡ Toru Furukawa,¶ Masao Ono,* Takuya Moriya,* Kiyoshi Ito,‖ Haruo Saito,† Tadashi Ishibashi,† Shoki Takahashi,† Shogo Yamada,† and Hironobu Sasano*

From the Departments of Pathology, Radiology,† Molecular Pathology,¶ and Gynecology,‖ Tohoku University School of Medicine, Sendai; and the Division of Toxicology‡ and the Biological Safety Research Center;§ National Institute of Health Sciences, Tokyo, Japan*

Estrogen has been postulated to be involved in inhibition of vascular smooth muscle cell (VSMC) proliferation mainly via estrogen receptor (ER), but the detailed mechanism has remained primarily unknown. Therefore, in this study, microarray analysis was used in two types of cultured human VSMCs: one positive for ERα, and the other for ERβ, which were treated by estrogens to detect the estrogen-responsive genes. We also used quantitative reverse transcriptase-polymerase chain reaction (RT-PCR) to evaluate mRNA levels of selective target gene (TG) in these cells. We further studied whether the TG product was involved in inhibition of proliferation using small interfering RNA (siRNA) of the TG transfection. We subsequently used quantitative RT-PCR and *in situ* hybridization analysis to evaluate the expression of these gene products in human aorta. E4F1, a possible inducer of cell growth arrest, was markedly increased only in ERα-positive VSMCs by estrogens in both microarray and RT-PCR analyses. Blocking of E4F1 using siRNA suppressed estrogenic inhibition of ERα-positive VSMC proliferation. E4F1 mRNA was abundant in premenopausal female aorta with mild atherosclerotic changes. E4F1 is therefore considered one of the estrogen-responsive genes involving ERα-mediated inhibition of VSMC proliferation and may play an important role in estrogen-related atheroprotection of human aorta. *(Am J Pathol 2004, 165:2019–2031)*

Estrogen has been proposed as a cardioprotective agent.[1] However it is also true that the significance of hormone replacement therapy has remained controversial because recent randomized controlled trials failed to show protective effects of hormone replacement therapy in reducing the risk of coronary artery disease and instead revealed undesirable side effects such as an increment of breast cancer incidence.[2–4] Results of experimental, clinical, and epidemiological studies have, however, also demonstrated that estrogen is predominantly involved in the suppression of development of atherosclerosis.[2,5,6] Therefore, it is still very important to examine the detailed mechanisms of estrogenic actions especially in relation to its atheroprotective effects in the human cardiovascular system.

Estrogens have been considered to exert direct anti-atherogenic effects through an initial interaction with estrogen receptor (ER) in vascular smooth muscle cells (VSMCs) in addition to various systemic estrogenic effects. Results of recent studies demonstrated that there are two subtypes of ERs, ERα and ERβ.[7,8] The presence of both ERα and ERβ has been also reported in the vascular wall of cardiovascular systems in human and various experimental animals.[9] Between both ERs, ERα has been considered to be important for anti-atherogenic effects of estrogen in the great majority of the cases.[9–13] However, the detailed genomic mechanisms of estrogen-ERα actions in inhibition of VSMC proliferation remain virtually unknown. Especially the target gene (TG) induced by estrogen, ie, estrogen-responsive gene, has not been examined in the human cardiovascular system.

Supported in part by Health and Labor Sciences Research Grants for Risk Analysis Research on Food and Pharmaceuticals (H13-Seikatsu-013) from the Ministry of Health, Labor, and Welfare of Japan.

Accepted for publication August 25, 2004.

Address reprint requests to Yasuhiro Nakamura, M.D., Department of Pathology, Tohoku University School of Medicine, 2-1 Seiryo-machi, Aoba-ku, Sendai, 980-8575 Japan. E-mail: nakamura@patholo2.med.tohoku.ac.jp.

Table 1. Primer Sequences Used in RT-PCR Analysis for VSMC Characterization

cDNA	Sequence	Size (bp)	Reference no.
ERα	Forward 5′-AAGAGCTGCCAGGCCTGCC-3′ Reverse 5′-TTGGCAGCTCTCATGTCTCC-3′	167	56
ERβ	Forward 5′-GCTCAATTCCAGTATGTA-3′ Reverse 5′-CCTGGTGTAAAAACGTGA-3′	241	57
GAPDH	Forward 5′-TGAACGGGAAGCTCACTGG-3′ Reverse 5′-TCCACCACCCTGTTGCTGTA-3′	307	58

Recently, expression profiling analysis using cDNA microarray technology has been demonstrated to provide very important information as to the elucidation of the scheme of estrogen-signaling and improvement of clinical decisions in ERα-positive breast cancer.[14] A number of investigators also identified several novel estrogen-responsive genes using a cDNA microarray method in other tissues and cancer cells.[14,15] However, there has been little information regarding estrogen-responsive genes involving anti-atherogenic effects induced by estrogens in the human cardiovascular system. Therefore, in this study, we first screened the estrogen-responsive gene involving inhibition of VSMC proliferation using a microarray in a cell line derived from ERα-positive human VSMCs. We then used quantitative reverse transcriptase-polymerase chain reaction (RT-PCR) to evaluate the expression level of this TG mRNA in both dose- and time-dependent manners to further confirm the results of microarray analysis. We also examined whether the TG detected in ERα-positive VSMCs can be also induced by estrogens in ERβ-positive VSMCs. Double-stranded RNAs (dsRNAs) have been recently reported to be remarkably effective at suppressing specific gene expression in various kinds of cells by a pathway involving RNA interference (RNAi) through small interfering RNAs (siRNAs).[16–18] Therefore, we used this procedure to confirm whether the gene products derived from the TG detected in microarray analysis were associated with estrogenic inhibition of cell proliferation in ERα-positive cells.

It then becomes very important to study the expression of the genes detected by microarray analysis in human VSMCs to obtain their clinical relevance. We therefore examined the expression levels of the above TG in VSMCs of human abdominal aorta obtained by autopsy using both quantitative RT-PCR and the *in situ* hybridization method. We then correlated these findings with the degree of atherosclerosis, sex, ERα expression levels, and other features of the patients for further characterization of the findings.

Materials and Methods

Cell Culture and Characterization

Two types of human VSMCs, ie, HUVS-112D (derived from human umbilical cord; CRL-2481), and T/G HA-VSMC (derived from human aorta; CRL-1999) were commercially obtained from American Type Culture Collection (Manassas, VA). They were cultured in a 75-cm^2 flask with F12-K medium (American Type Culture Collection) containing 5% fetal bovine serum (FBS) at 37°C in a 5% CO_2 atmosphere. We first characterized these cell lines using several methods, such as morphological, immunohistochemical, and microarray analyses described below. In addition, we examined whether these cells expressed both ERs, especially ERα, using quantitative RT-PCR and Western blot analysis in combination with semiquantification, as described below.

Quantitative RT-PCR

Total RNA was extracted from both VSMCs in 1 ml of TRIzol reagent (Invitrogen, Carlsbad, CA) followed by a phenol-chloroform phase extraction and isopropanol precipitation. The Superscript Preamplification System RT kit (Life Technologies, Inc., Grand Island, NY) was used in the synthesis and amplification of complementary DNA (cDNA). cDNA was synthesized from total RNA (2 μg) using 25 ng/μL of Oligo $(dT)_{12-18}$ Primer (Life Technologies Inc., Gaithersburg, MD) on a PTC-200 Peltier thermal cycler DNA engine (MJ Research Inc., Watertown, MA). To test for the presence of genomic DNA contamination, we performed the RT step in the absence of Superscript II RNase H^- reverse transcriptase (Life Technologies, Inc.) followed by PCR. RT-PCR products lacking reverse transcriptase in the initial RT step were run on an ethidium bromide-stained 2% agarose gel. No band was observed in these samples (data not shown). The resulting cDNA was used as a template for real-time PCR. Real-time PCR was performed with the Light Cycler System (Roche Diagnostics GmbH, Mannheim, Germany) using the DNA binding dye SYBR Green I (Roche Diagnostics GmbH) for the detection of PCR products. Primers are summarized in Table 1. As a positive control, T-47D human breast cancer cells were used for ERα and ERβ.[19] Negative control experiments lacked cDNA substrate to check for the presence of exogenous contaminant DNA. No amplified products were detected under these conditions. The mRNA levels for both ERs in each VSMC are summarized as a ratio of glyceraldehyde-3-phosphate dehydrogenase (GAPDH), and evaluated as a ratio (%) compared with that of each control cDNA, which were synthesized from each PCR products and purified by using the pGEM-T Easy vector. The detailed procedures above were previously described in detail.[20] The analyses with real-time PCR were triplicated.

Western Blot Analysis

The procedures were based on these reported previously.[21] The above VSMCs were washed with ice-cold phosphate-buffered saline (PBS) and then lysed in a triple detergent buffer containing 50 mmol/L Tris-HCl (pH 8.0), 150 mmol/L NaCl, 0.02% sodium azide, 0.1% sodium dodecyl sulfate, 100 μg/ml phenylmethyl sulfonyl fluoride, 1 μg/ml aprotin, 1% Nonidet P-40, and 0.5% sodium deoxycholate. A Protein Assay Rapid Kit (Wako, Osaka, Japan) and a SpectraMax 190 microplate reader (Molecular Devices Corp., Sunnyvale, CA) were used to determine the concentration of protein according to the manufacturers' instructions. A Western blot analysis was performed using 60 μg of each protein. After optimizing the conditions of experiments, 60 μg of protein samples were denatured at 95°C in Tris/glycine/sodium dodecyl sulfate buffer (25 mmol/L Tris, 192 mmol/L glycine, 0.1% sodium dodecyl sulfate, pH 8.3) and electrophoresed at 25-mA constant current through a 10 to 20% polyacrylamide gradient gel (Bio-Rad, Hercules, CA). The proteins in the gel were electrophoretically transferred to a polyvinylidene difluoride membrane (Clear Blot Membrane-P; ATTO Co. Ltd., Tokyo, Japan). Nonspecific binding sites were blocked by immersing the membrane in 5% skim milk (Becton Dickinson and Company, NJ) for 1 hour at room temperature, washed twice in 0.05% Tween 20 and PBS (PBS-T), and then incubated with ERα polyclonal antibody (Santa Cruz Biotechnology, Inc., Santa Cruz, CA) or control IgG overnight at 4°C. After washing in PBS-T, membranes were incubated for 1 hour with horseradish peroxidase-conjugated anti-mouse IgG (Amersham), and the target protein was detected using the ECL Western blotting detection reagent (Amersham). Equal loading of protein in each lane was confirmed by probing the membrane with anti-human β-actin monoclonal antibody (Sigma, St. Louis, MO). The relative amounts of ERα and β-actin protein levels for each band were standardized to the relative OD units obtained by an Image Gauge system (Fuji Photo Film Co. Ltd., Minamishinagawa, Kanagawa, Japan). In addition, the relative amount of ERα protein was adjusted by the β-actin protein level, and then evaluated as a ratio (%) to untreated MCF-7 cell lines.[22] The analyses were also triplicated.

GeneChip Microarray Assay

Estrogen Treatment

The two types of VSMC cells described above were seeded in a 75-cm^2 flask at an initial concentration of 100,000 cells/flask with F12-K medium (American Type Culture Collection) containing 5% FBS and cultured until a subconfluent state was obtained. The medium was then replaced with FBS-free and phenol red-free medium (modified Eagle's medium) (Sigma) to arrest the cell growth. After 24 hours, the medium was replaced again with phenol red-free and FBS-free medium in the presence of estrogen (10 nmol/L) or vehicle (0.1% ethanol). After incubation for 8 hours, the cells were subsequently subjected to total RNA extraction for microarray analysis. Total RNA was prepared using TRIzol reagent (Invitrogen) according to the manufacturer's instructions. RNA was further purified using RNeasy columns (Qiagen, Valencia, CA) and treatment with ribonuclease-free deoxyribonuclease I (Qiagen).

Labeling

Isolated total RNA was labeled as described in the Affymetrix (Santa Clara, CA) GeneChip Expression Analysis Technical Manual (revision 3). The labeling is performed in two steps. In the first step, double-stranded cDNAs (ds-cDNAs) were synthesized from total RNA by reverse transcriptase reaction with SuperScript Reverse Transcriptase II (Life Technologies) and an oligo (dT) primer linked to a T7 RNA polymerase-binding site sequence and second strand synthesis reaction with *Escherichia coli* DNA polymerase, DNA ligase, and RNaseH. In the second step, the resulted ds-cDNAs were used as templates to produce biotin-labeled cRNA (the target) using T7 RNA polymerase in the presence of biotinylated UTP and CTP (Enzo Diagnostics, Farmingdale, NY). The biotin-labeled cRNAs were fragmented in fragmentation buffer and used for the preparation of target solution.

GeneChip Genome Array Hybridization

Fragmented targets are combined with control oligomer (Control Oligo B2, Affymetrix) and control cRNAs (Eukaryotic Hybridization Control kit, Affymetrix) in a hybridization buffer (100 mmol/L MES, 1 mol/L Na^+, 20 mmol/L ethylenediaminetetraacetic acid, 0.01% Tween 20). Each target was hybridized to HGU133A using protocols described in the Affymetrix Expression Analysis Technical Manual.

Data Analysis

The procedure was basically based on the previously reported study.[23] The fluorescent signals on the slides were scanned by a GeneArray scanner (Affymetrix) and further data processing was performed using Microsoft Excel software (Microsoft, Seattle, WA). Image analysis was performed using Microarray Suite 5.0 software (Affymetrix). In this study, the ratios represented the values changed by 10 nmol/L E_2 treatment compared to control values. The values obtained from each experiment were log transformed and normalized so that the median log-transformed ratio equaled zero. To confirm the estrogen-related changes in gene expression obtained from microarray analysis, we independently repeated the same experiment twice and the differences were calculated. To further maintain reproducibility, we also selected for further analysis only those genes in which the difference of expression levels at the same condition in two separate experiments did not exceed more than 2.5-fold in further analysis. The average ratios yielded by these independent experiments were then used to denote the gene expression levels. As the average ratios increased more than twofold by both of duplicated 10 nmol/L E_2 treatment

Table 2. The Sequence Information of Primers, siRNA, and Probes for *in Situ* hybridization for Target Gene (E4F1)

Primers for RT-PCR	Forward	5′-ACACCACACAGGCGAGAA-3′
	Reverse	5′-TCCTCAGACACCAGCAACT-3′
Gene-specific sequences for siRNA	Sense	5′- AAGCTCTACAAGACCATTGCC-3′
	Anti-sense	5′-AAGCTCTACAAGACCATTGCC-3′
Gene-specific probes for *in situ* hybridization	Anti-sense	5′-CCACGGAGATCATCGAGGGCACCCAGACAGAGGTGGACAGCCACATCATG-3′
	Sense	5′-CATGATGTGGCTGTCCACCTCTGTCTGGGTGCCCTCGATGATCTCCGTGG-3′

It was determined that the target gene in this study was E4F1 by microarray analysis The reason for this determination was described in detail in the Results section.

were considered to have been up-regulated when compared to control values. In this study, among the genes detected in microarray analysis, we regarded a gene that was up-regulated and was significantly associated with inhibition of cell growth in ERα-positive cells as the TG in this study. In an analysis of the function of these detected genes, we used the homepage of HUGO Human Gene Nomenclature Committee (*http://www.gene.ucl.ac.uk/nomenclature/*) for further clarification. We then examined whether there was an estrogen-responsive element (ERE) in the promoter region of TG by analyzing 10,000 bp upstream of the transcription start sites for TG with sequence information of chromosome mapping provided by the above homepage.

Real-Time PCR for TG mRNA

Estrogen Treatment

The ERα-positive cells were seeded in a 75-cm^2 flask at an initial concentration of 100,000 cells/flask with F-12K medium containing 5% FBS and cultured until a subconfluent state was obtained. The medium was then replaced with phenol red-free and FBS-free medium to arrest the cell growth. After 24 hours, the medium was replaced again with FBS-free F12-K medium with E_2 (100 pmol/L, 10 nmol/L), E_2 (10 nmol/L) with ICI 182780 (1 μmol/L; Tocris, Ballwin, MO), tamoxifen (TAM, Sigma) alone (10 nmol/L), raloxifene (RAL, Sigma) alone (10 nmol/L), or vehicle. In addition, after pretreatment of the cells with inhibitors of RNA transcription, actinomycin D (ACD) (1 μmol/L, Sigma), or protein translation (Sigma), cycloheximide (CHX) (1 μmol/L, ICN Biomedicals Inc.), other two flasks were replaced again with FBS-free medium with E_2 (10 nmol/L). After incubation for 8 hours, the cells were subsequently subjected to total RNA extraction for real-time RT-PCR analysis described above for target product mRNA expression. In addition, the cells were also incubated for 24 hours and 48 hours, respectively, with E_2 alone (10 nmol/L) or vehicle and also subsequently subjected to total RNA extraction for real-time RT-PCR analysis described above for expression levels of TG product mRNA. The mRNA levels for target product in each VSMC are summarized as a ratio of GAPDH, and evaluated as a ratio (%) compared with that of each control cDNA, which were synthesized from each PCR product and purified by using the pGEM-T Easy vector. The procedures were also previously described in detail.[20] As a contrast, we also examined the relative expression levels of TG products mRNA treated with E_2 (100 pmol/L, 10 nmol/L) or vehicle for 8 hours, and treated with E_2 (10 nmol/L) or vehicle for 24 hours and 48 hours in ERβ-positive cells. The analyses with real-time PCR were triplicated by using three flasks per treatment or nontreatment. The sequence information of primers for TG is shown in Table 2.

siRNA Preparation, Transfection, and Cell Count Assay

siRNAs corresponding to the TG mRNAs designed with 5′ phosphate, 3′ hydroxyl, and two base overhangs on each strand were synthesized and transfected to the ERα-positive VSMCs. The ERα-positive cells were seeded in a 25-cm^2 flask at an initial concentration of 50,000 cells/flask with F-12K medium containing 5% FBS and cultured until a subconfluent status was achieved. The medium was then replaced with phenol red-free and FBS-free medium to arrest the growth. After 24 hours, transfections of siRNA for endogenous gene targeting were performed with TransMessenger transfection reagent (Qiagen). The TG siRNA (2 μg per flask) was condensed with 4 μl of Enhancer R and formulated with 8 μl of TransMessenger reagent, according to the manufacturer's instructions. The transfection complex was added directly to the cells; it was replaced with phenol red-free medium containing 5% dextran-coated charcoal-stripped FBS (DCC-FBS) with E_2 (10 nmol/L), TAM (10 nmol/L), RAL (10 nmol/L), or vehicle (0.1% ethanol) after 3 hours. After incubation for 48 hours, we then measured the number of cells in each sample as described above. We also examined the number of cells treated with E_2 (10 nmol/L) or vehicle (0.1% ethanol) with transfection of negative control siRNA and treated by E_2 (10 nmol/L), TAM (10 nmol/L), RAL (10 nmol/L), or vehicle into both ERα-positive cells. After incubation for 48 hours, the cells were trypsinized and suspended. We then used Cell Counting Kit-8 system (Wako) for measurement of the number of cells in each sample. As a contrast, we also examined the number of cells treated with E_2 (10 nmol/L) or vehicle with transfection of TG or negative control siRNA in ERβ-positive cells treated by E_2. The effective ratio of transfection into the cells was more than 80% by using fluorescein-labeled negative control siRNA before transfection of the TG siRNA (data not shown). The sequence information of siRNA for TG is shown in Table 2.

Quantitative RT-PCR Analysis for mRNA of the TG Expression in Human Aorta

Human abdominal aortae without hormone therapy were collected at the time of autopsy performed in Tohoku University Hospital (Sendai, Japan) within 2 hours postmortem from 22 patients (6 male, 6 premenopausal female, 10 postmenopausal female; mean, 52.2 ± 5.9 years of age). The Ethics Committee at Tohoku University School of Medicine approved the research protocol for this study. Aortic specimens were tentatively classified into the following five groups as previously described,[20] A, B, C, D, and E based on the sex of the deceased patient, degree of atherosclerosis, and status of menstruation (group A: male, normal or mild atherosclerosis, corresponding to group I to III in the AHA classification; group B: male, advanced atherosclerosis, corresponding to group IV to VI in the AHA classification; group C: premenopausal female, normal or mild atherosclerosis; group D: postmenopausal female, advanced atherosclerosis; and group E: postmenopausal female, mild atherosclerosis). The distribution of the cases among these groups is summarized as follows: A, three cases; B, three cases; C, six cases; D, six cases; and E, four cases. The adventitia and fat tissues around the aorta were immediately and carefully removed using clean surgical scissors and forceps at the time of autopsy. After this procedure, these specimens were immediately frozen in liquid nitrogen and stored at −80°C until use and also subsequently subjected to total RNA extraction for real-time RT-PCR analysis described above for expression levels of TG product mRNA and the correlation of ERα mRNA abundance in those samples. The mRNA levels for target product and ERα in each sample are summarized as a ratio of GAPDH, and evaluated as a ratio (%) compared with that of each control cDNA, which were synthesized from each PCR product and purified by using the pGEM-T Easy vector, as described above.

In Situ *Hybridization Study for the TG mRNA Expression in Human Aorta*

Unstained and duplicated, 5-μm-thick, formalin-fixed, paraffin-embedded human aorta sections were mounted onto clear glass slides (Matsunami, Tokyo, Japan) and processed using the RiboMap *in situ* hybridization kit (Ventana Medical Systems, Tucson, AZ) on the Ventana Discovery (Ventana Medical Systems) automated *in situ* hybridization instrument. *In situ* hybridization step protocols after the deparaffinization step were designed based on the standard protocol described in the manufacture's RiboMap application note. The first fixation step was performed using formalin-based RiboPrep reagent (Ventana Medical Systems) for 30 minutes at 37°C. The reacted sections were then acid-treated using hydrochloride-based RiboClear reagent (Ventana Medical Systems) for 10 minutes at 37°C. The slides were subsequently processed for the protease digestion using ready-to-use a protease 2 reagent. The sections were incubated for hybridization with the anti-sense riboprobe (2 ng/slide) using RiboHybe hybridization buffer (Ventana Medical Systems) for 6 hours at 37°C after a denaturing step for 6 minutes at 70°C. After stringency wash step using 2× RiboWash (equivalent to 0.2× standard saline citrate, Ventana Medical Systems) for 6 minutes at 42°C, the second fixation step was performed using RiboFix reagent for 20 minutes at 37°C followed by incubation of biotin-labeled anti-digoxigenin antibody (Sigma) for 30 minutes at 37°C. After streptavidin-alkaline phosphatase conjugate incubation for 16 minutes at 37°C, the signal was detected automatically using the BlueMap NBT/BCIP substrate kit for 4 hours at 37°C. Finally, the sections were counterstained with Kernechtrot as a marker stain and covered with a glass coverslip. We also used double immunostaining with diaminobenzidine (DAB) for ERα using a monoclonal antibody (Novocastra Laboratories, Newcastle, UK) and Vector-blue for α-smooth muscle actin using a monoclonal antibody (DAKO Corp., Carpinteria, CA), respectively, in adjacent tissue sections to further characterize these positive cells in the human aorta of the cases positive for the target mRNAs. We also used a monoclonal antibody against CD31 antigen (DAKO) for endothelial cells and a monoclonal anti-human macrophage antibody (PG-M1, DAKO) for macrophages in adjacent tissue sections for further characterization. In addition, we performed labeling index (LI), a quantitative value that evaluates the number of TG mRNA-positive cells present in VSMCs of the aortic neointima and media.[24] After determining the areas of evaluation by simultaneous observation using a multiheaded light microscopy, three authors (T.S., M.S., and H.S.) independently evaluated 100 VSMCs. When interobserver differences were less than 5%, the mean value was determined as the LI. When interobserver differences were greater than 5%, the three aforementioned authors above re-evaluated the discrepant immunostained slides simultaneously using a multiheaded light microscope, after which the mean value was obtained. The sequence information of probes for *in situ* hybridization for TG is shown in Table 2.

Statistical Analysis

Values for all results are shown as mean ± SE of means (SEM). For comparisons between two groups, we used one-way analysis of variance followed by unpaired *t*-test. To examine the correlation of the two factors, we used a correlation coefficient (r) and a regression equation. A P value less than 0.05 was considered significant in this study.

Results

Characterization of Two VSMC Cell Lines

Results are summarized in Figures 1 and 2. We confirmed that these cells were positive for α-smooth muscle actin immunoreactivity but both of these cell lines represented relatively dedifferentiated VSMCs on the basis of their morphological features and expression of specific markers such as caldesmon, α-tropomyosin, and others (data not shown). In RT-PCR analysis, HUVS-112D cells

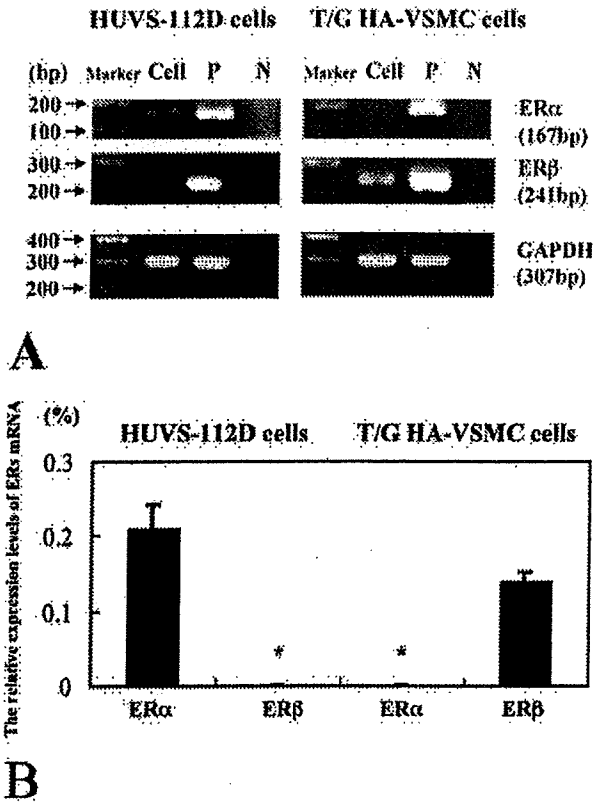

Figure 1. A: Results of real-time RT-PCR analysis for ERα and ERβ in two cultured human VSMC lines (HUVS-112D and T/G HA-VSMC), positive controls, and negative controls. Cell, each type of cultured VSMC; P, positive controls (T-47D breast cancer cell lines); N, negative controls (no cDNAs). T-47D breast cancer cell lines were both positive for ERα and ERβ. Negative controls yielded no bands for both ERα and ERβ. In HUVS-112D cells, only the bands of ERα were detected, whereas only the bands of ERβ were detected in T/G HA-VSMC cells. **B:** The relative mRNA expression levels for both ERs in two types of VSMC lines. The data for RT-PCR were adjusted by ratios (%) of GAPDH mRNA compared with that of each control cDNA, which were synthesized from each PCR product and purified by using the pGEM-T Easy vector. *, PCR products were not detected and the relative expression levels resulted in zero.

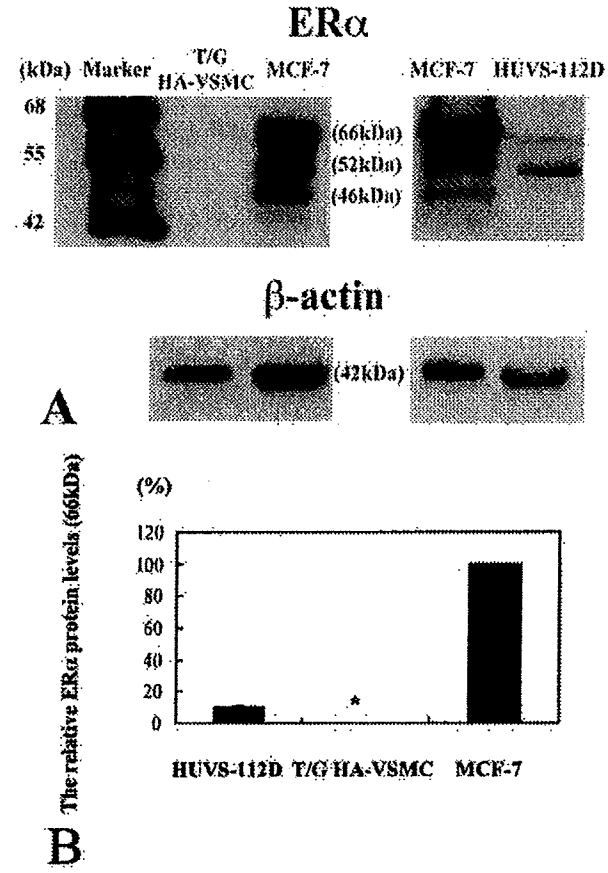

Figure 2. A: Western blot analysis of ERα and β-actin in HUVS-112D cells, T/G HA-VSMCs, and MCF-7 cells. Total protein was extracted and 60 μg of protein from each cell was loaded. Western blot analysis demonstrated both the full-length ERα protein (66 kd) in HUVS-112D and MCF-7 cells, but not in T/G HA-VSMCs. In addition, both HUVS-112D and MCF-7 cells were also positive for the exon 7 deletion variant of ERα protein (52 kd). On the other hand, MCF-7 cells were positive for another splicing variant of ERα protein (46 kd). **B:** The relative protein expression levels for the full-length ERα protein (66 kd) in two types of VSMC lines. The results were evaluated as a ratio (%) compared with that of untreated MCF-7 cells. *, Bands of protein were not detected and the relative expression levels resulted in zero.

were positive only for ERα (0.21 ± 0.03%, adjusted by ratios of GAPDH mRNA), and T/G HA-VSMCs were positive only for ERβ (0.14 ± 0.01%, adjusted by ratios of GAPDH mRNA) (Figure 1).

In Western blot analysis, only HUVS-112D cells were positive for the full-length ERα protein (66 kd) (10.4 ± 0.8%, adjusted by ratios of β-actin protein compared to the ratio of MCF-7 cells) (Figure 2). In addition, HUVS-112D cells were also positive for the exon 7 deletion variant of ERα protein (52 kd), which is known to be expressed in both human VSMCs and MCF-7 cells, and known to inhibit transcriptional activation of wild-type ERs with little transcriptional activity by itself (Figure 2).[25,26] On the other hand, MCF-7 cells were also positive for another splicing variant of ERα protein (46 kd) (Figure 2).[27]

Gene Chip Microarray Assay

Table 3 shows the 12 genes that demonstrated expression ratios of above 2.0 after 8 hours of duplicated 10 nmol/L E_2 treatment of ERα- and/or ERβ-positive cells. Among these genes, E4F transcription factor 1, ie, E4F1 was detected in HUVS-112D cells (ERα-positive cells), and its expression was associated with the second highest ratios by duplicated 10 nmol/L E_2 treatment (2.4-fold) (Table 3). In addition, among the detected genes, only E4F1 has been reported to inhibit cell growth and cell-cycle progression.[28-33] In addition, more than 20 half-EREs in the promoter region of E4F1 were detected in this search (data not shown). Therefore we further examined the features of E4F1 as an estrogen-responsive gene in human VSMCs and whether E4F1 was associated with estrogenic inhibition of ERα-positive cell proliferation using quantitative RT-PCR, and siRNA transfection assay described above. In addition, we examined the expression levels of E4F1 mRNA in human abdominal aorta using both quantitative RT-PCR and *in situ* hybridization. In this study, E4F1 was not detected in T/G HA-VSMC cells (ERβ-positive cells). In addition, among the genes detected by microarray analysis, the gene associated with inhibition of VSMC proliferation was not demon-

Table 3. Genes Up-Regulated by Estrogen Treatment for 8 Hours in Cultured VSMCs

Cell lines	Approved gene symbols	RefSeq accession numbers	Ratios
HUVS-112D (ERα-positive)	INPP4B	NM_003866	2.8
	E4F1	NM_004424	2.4
	CKLF	NM_016326	2.2
	RYR3	NM_001036	2.2
	PLAG1	NM_002655	2.1
T/G HA-VSMC (ERβ-positive)	RFP2	NM_005798	2.5
	CPM	NM_001874	2.4
	EGR3	NM_004430	2.3
	POFUT1	NM_015352	2.3
	ADPRTL2	NM_005484	2.1
	HAP1	NM_177977	2.1
	RBM12	NM_152838	2.1

Ratios represents the mean ratios of expression levels of each gene mRNA between biologically duplicated experiments with estrogen and without estrogen.

strated in ERβ-positive VSMCs according to the results of our research.

E4F1 mRNA Expression in VSMCs by Estrogen Treatment

E_2 significantly increased E4F1 mRNA levels of ERα-positive VSMCs compared to controls (131.9 ± 5.9% by E_2 100 pmol/L, 267.0 ± 19.7% by E_2 10 nmol/L, respectively; $P < 0.05$) (Figure 3A). In addition, E_2 with CHX also significantly increased those of ERα-positive VSMCs compared to controls (172.4 ± 20.3%, $P < 0.05$) (Figure 3A). However, E_2 with ICI 182780, TAM, RAL, and E_2 with ACD suppressed expression of these mRNAs (33.4 ± 0.1% by E_2 10 nmol/L with ICI 182780 1 μmol/L, 63.5 ± 16.9% by TAM 10 nmol/L, 32.3 ± 1.8% by RAL 10 nmol/L, 48.5 ± 10.6% by E_2 10 nmol/L with ACD 1 μmol/L, respectively; $P < 0.05$) (Figure 3A). In addition, E4F1 mRNA levels of ERα-positive VSMCs were the highest at 8 hours after E_2 10 nmol/L treatment compared to control (267.0 ± 19.7%) (Figure 3C). However, none of E_2 significantly increased or inhibited E4F1 mRNA levels of ERβ-positive VSMCs compared to controls (Figure 3, B and D). In summary, results of quantitative RT-PCR analyses also demonstrated that E4F1 is one of the genes induced by estrogen via ERα, but not via ERβ, in our cultured human VSMCs.

E4F1 siRNA Transfections and Cell Proliferation Assay

We confirmed the down-regulation of E4F1 mRNA levels in the cells by transfection of E4F1 siRNAs using RT-PCR (data not shown). After transfection of negative control siRNA, all E_2 and estrogen receptor modulators (SERMs) used in this study significantly inhibited proliferation of ERα-positive VSMCs compared to controls (20.0 ± 2.2% by E_2 10 nmol/L, 28.2 ± 1.0% by TAM 10 nmol/L, and 12.0 ± 0.2% by RAL 10 nmol/L, respectively; $P < 0.05$) (Figure 4A). In addition, TAM and RAL significantly inhibited proliferation of ERα-positive VSMCs compared to controls (30.7 ± 1.6% by TAM 10 nmol/L, and 13.7 ± 1.0% by RAL 10 nmol/L, respectively; $P < 0.05$) after transfection of E4F1 siRNA (Figure 4A). However, E_2 with transfection of E4F1 siRNA did not suppress the proliferation of ERα-positive VSMCs (Figure 4A). In addition, none of the agents examined in this study significantly inhibited the cell proliferation of ERβ-positive VSMCs compared to controls by transfection of both E4F1 siRNA and negative control siRNA (Figure 4B). In summary, siRNA analysis indicated that E4F1 may be associated with inhibition of VSMC proliferation through ERα not ERβ in our cultured VSMCs.

E4F1 mRNA Expression in Human Aorta

The relative abundance of E4F1 mRNA determined by real-time PCR analysis was significantly higher in the premenopausal female aorta with a mild degree of atherosclerotic changes (group C, 2.22 ± 0.37%) than in the male aorta with a mild degree of atherosclerosis (group A, 0.09 ± 0.05%), with a severe degree of atherosclerosis (group B, 0.31 ± 0.27%), and in the postmenopausal female aorta with a severe degree of atherosclerosis (group D, 0.24 ± 0.12%) ($P < 0.05$) (Figure 5B). In addition, there was a significant positive correlation between expression levels of ERα mRNA and relative abundance of E4F1 mRNA expression in female aorta ($y = 0.571 + 1.641 * x$, $r = 0.65$; $P < 0.05$) (Figure 5C). In addition, there was a significant inversed correlation between ages of the patients and the abundance of E4F1 mRNA expression in female aorta ($y = 2.482 - 0.026 * x$, $r = -0.575$; $P < 0.05$) (data not shown). However, no significant correlations were detected between relative abundance of E4F1 mRNA and ages and degree of atherosclerosis in male aorta (data not shown). In summary, results of quantitative RT-PCR in human aorta demonstrated that E4F1 was markedly expressed in premenopausal female aorta in an early stage of atherosclerosis with abundant ERα.

In Situ *Hybridization Study for E4F1 mRNA Expression in Human Aorta*

Expression of E4F1 mRNA products were markedly present in ERα-positive VSMCs at neointima of aorta in

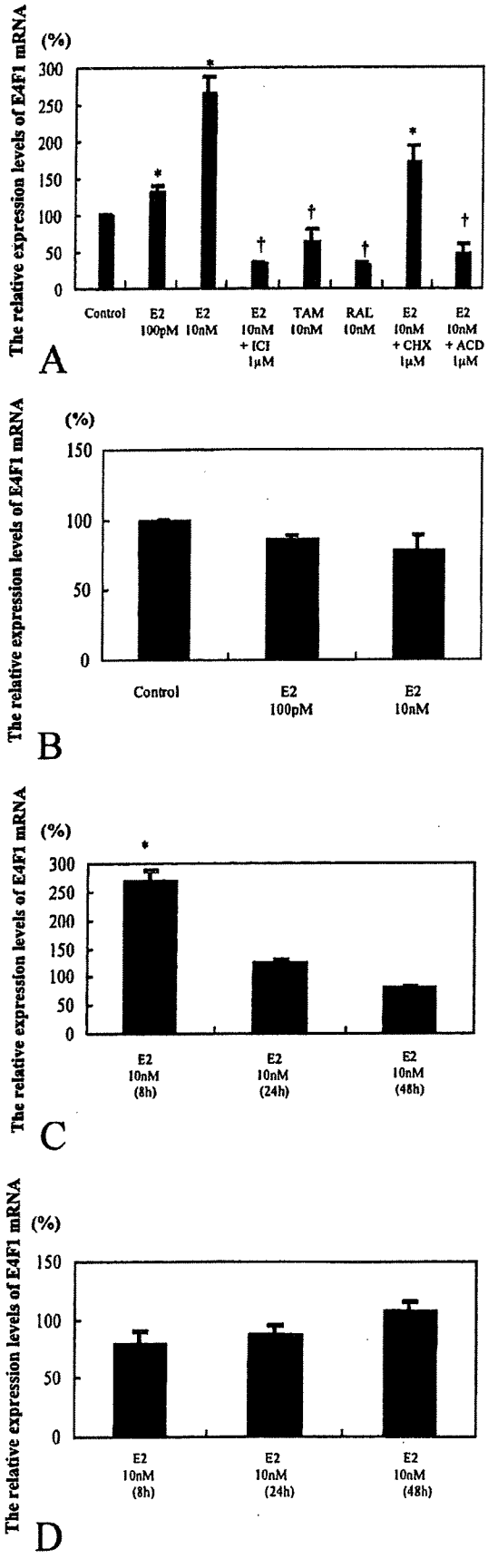

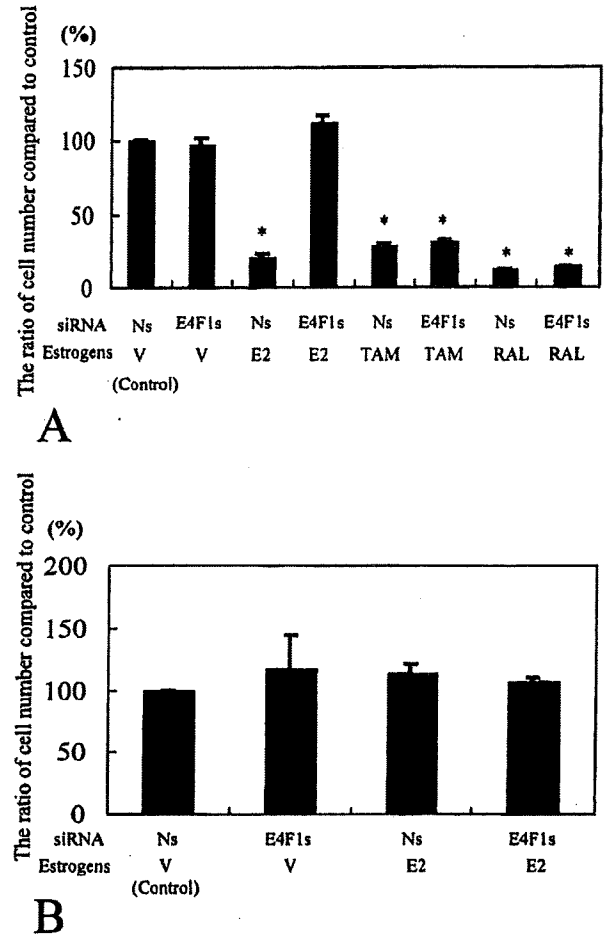

Figure 4. A: The relative levels of cell numbers in HUVS-112D cells (ERα-positive cells) among cells treated with vehicle (control), estrogen (E_2) alone (10 nmol/L), tamoxifen (TAM; 10 nmol/L), raloxifene (RAL; 10 nmol/L), or vehicle (V; 0.1% ethanol) after transfection of E4F1 siRNA (E4F1s) or negative control siRNA (Ns). *, Significantly decreased compared to control; $P < 0.05$. **B:** The relative levels of cell numbers in T/G HA-VSMCs (ERβ-positive cells) among cells treated with vehicle (control), E_2 alone (10 nmol/L), or vehicle (V; 0.1% ethanol) after transfection of E4F1 siRNA (E4F1s) or negative control siRNA (Ns). *, Significantly decreased compared to control; $P < 0.05$.

group C. However, a very low level of expression of both E4F1 mRNA and ERα immunoreactivity was demonstrated in the nuclei of VSMCs of aorta in other groups. In addition, none of CD31-positive cells or PG-M1-positive cells demonstrated any hybridization signals of E4F1 mRNAs (data not shown). Figure 6 shows representative illustrations of an abdominal aorta specimen obtained from a 38-year-old woman with a mild degree of athero-

Figure 3. A: Results of real-time RT-PCR analysis for E4F1 in HUVS-112D cells (ERα-positive cells) among cells treated with vehicle (control), E_2 alone (100 pmol/L, 10 nmol/L), E_2 (10 nmol/L) with ICI 182780 (1 μmol/L), E_2 (10 nmol/L) with actinomycin D (ACD; 1 μmol/L), E_2 (10 nmol/L) with cycloheximide (CHX; 1 μmol/L), tamoxifen (TAM) alone (10 nmol/L), and raloxifene (RAL) alone (10 nmol/L), respectively, after 8 hours. **B:** Results of real-time RT-PCR analysis for E4F1 in T/G HA-VSMCs (ERβ-positive cells) among cells treated with vehicle (control), E_2 (100 pmol/L, 10 nmol/L) alone, respectively, after 8 hours. **C** and **D:** The relative levels of E4F1 mRNA expression in ERα-positive cells (**C**) and ERβ-positive cells (**D**) treated by E_2 alone (10 nmol/L) after 8, 24, and 48 hours compared to control (treated by vehicle). *, Significantly increased compared to control; †, significantly decreased compared to control; $P < 0.05$.

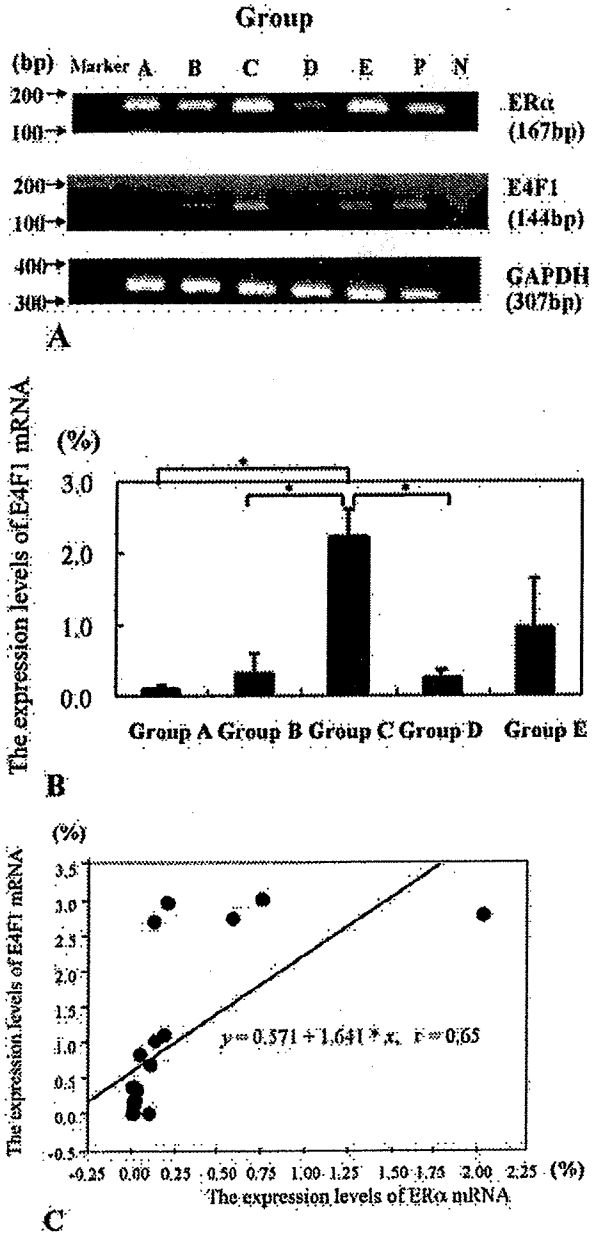

Figure 5. A: Results of real-time RT-PCR analysis for E4F1 in human aortas. Bands for PCR products were detected as specific single bands (167 bp for ERα, 144 bp for E4F1, and 307 bp for GAPDH). The amplified products were run on a 2% agarose gel stained with ethidium bromide. Representative photographs for these real-time RT-PCR gene products are illustrated. A, Aorta of a 32-year-old man with mild atherosclerotic change; B, Aorta of a 65-year-old man with severe atherosclerotic change; C, aorta of a 38-year-old premenopausal woman with mild atherosclerotic change; D, aorta of a 76-year-old postmenopausal woman with severe atherosclerotic change; E, aorta of a 71-year-old postmenopausal woman with mild atherosclerotic change; P, positive controls; N, negative controls. **B:** The results for mRNA expression levels for E4F1 (*, $P < 0.05$). **C:** Correlation between the levels of mRNA expression for ERα and E4F1 in 22 samples of human aorta. A significant correlation was detected ($y = 0.571 + 1.641x$; $r = 0.65$; $P < 0.05$).

sclerosis (group C). The number of E4F1 mRNA-positive cells in the neointima was significantly higher in the premenopausal female aorta with a mild degree of atherosclerotic changes (group C, 24.0 ± 2.0 LI) than in the male aorta with a mild degree of atherosclerosis (group A, 5.6 ± 0.5 LI), in the male aorta with a severe degree of atherosclerosis (group B, 3.2 ± 0.4 LI), in the postmenopausal aorta with a severe degree of atherosclerosis (group D, 2.4 ± 0.5 LI), and in the postmenopausal aorta with a mild degree of atherosclerosis (group E, 6.2 ± 1.5 LI) ($P < 0.05$) (Table 4). However, LI for E4F1 mRNAs in the media was not significantly different among these groups (Table 4). In summary, results of *in situ* hybridization study in human aorta demonstrated that E4F1 was markedly expressed in ERα-positive VSMCs present at neointima of premenopausal female aorta in an early stage of atherosclerosis.

Discussion

In this study, results of microarray and quantitative RT-PCR analyses all suggest that E4F1 is one of the genes induced by estrogen via ERα, but not via ERβ, in cultured human VSMCs. In addition, siRNA analysis demonstrated that E4F1 might be associated with inhibition of VSMC proliferation through ERα. Results of quantitative RT-PCR and *in situ* hybridization studies in human aorta further showed that E4F1 was markedly expressed in ERα-positive VSMCs present at neointima of premenopausal female aorta in an early stage of atherosclerosis.

In this study, we used duplicated microarray analyses as an initial screening. We then confirmed whether the gene was induced by estrogens or not by triplicated (using three flasks per treatment or nontreatment) quantitative RT-PCR. We then used siRNA assay for further examination of the findings. These findings all demonstrated that results of microarray analysis were consistent with those of RT-PCR, and the gene revealed by microarray analysis was actually involved in estrogenic inhibition of ERα-positive VSMC proliferation as demonstrated by the cell count assay with siRNA transfection.

E4F1 is well-known as a Krüppel-like family member.[28] The growth inhibitory activity of E4F1 has also been demonstrated to be associated with the posttranscriptional elevation of several cell-cycle regulatory proteins, including the CDK inhibitors $p21^{Waf1}$ and $p27^{Kip1}$ with reduced cdk2 and cdk4/6 activities, and with the down-regulation of cyclin A and cyclin E gene expression.[28–30] E4F1-induced cell-cycle arrest has been also reported to be enhanced by its interaction with the p53 transcription factor and hypophosphorylated pRb.[28,32,33] All of these findings above are consistent with the results of previous studies reported, and with inhibitory effects of estrogens on VSMC proliferation.[34]

Stimulation of responsive genes in response to estrogen is postulated to be mediated by the direct binding in which E_2-liganded ER binds directly to a specific sequence called an ERE and interacts directly with coactivator proteins and components of the RNA polymerase II transcription initiation complex which result in enhanced transcription.[35] This is also consistent with results of our computer-based search of ERE in the promoter region of E4F1. In addition, quantitative RT-PCR analysis in our present study also demonstrated that ACD suppressed estrogen-induced E4F1 mRNA expression,

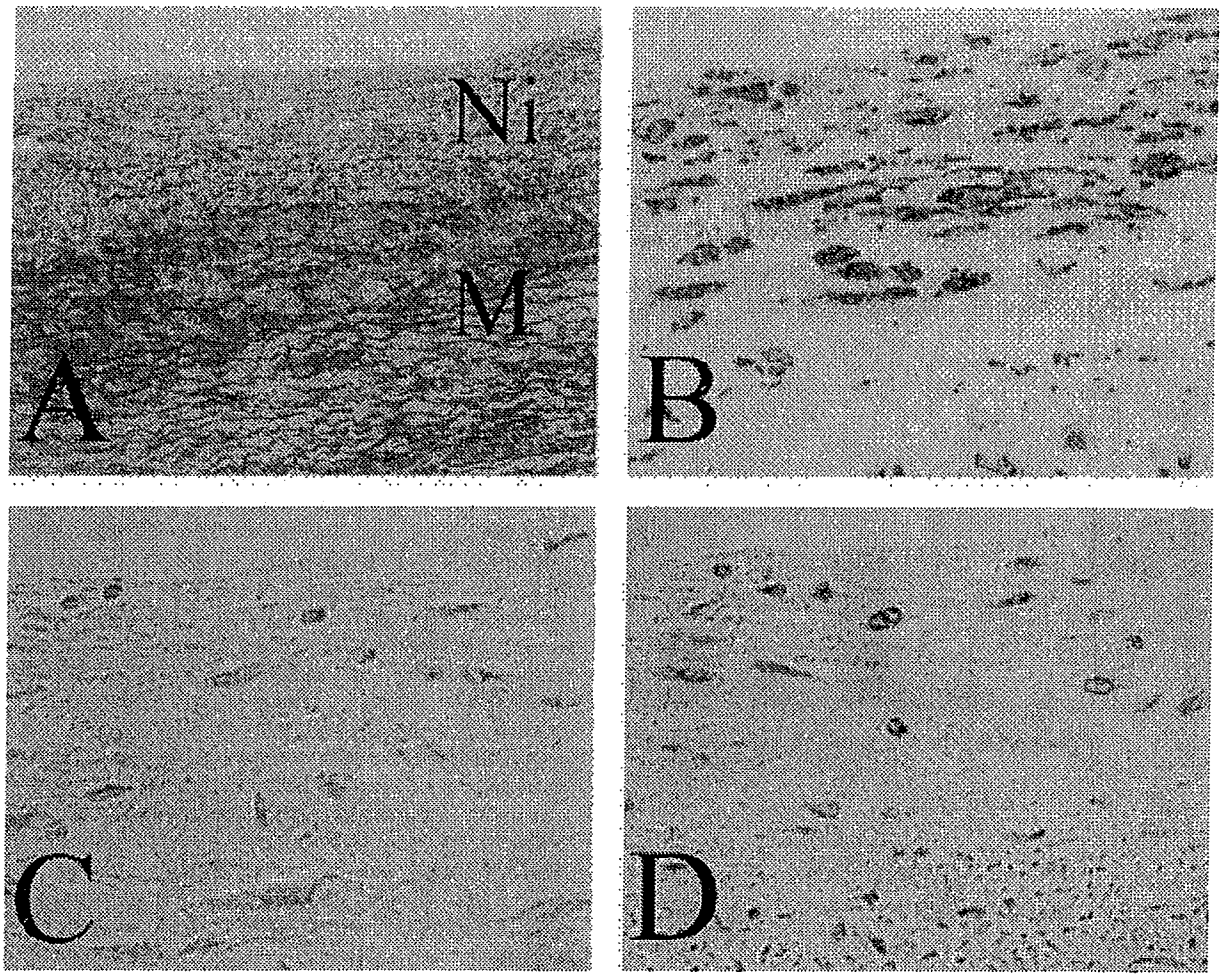

Figure 6. Modified Masson-Goldner's stains (**A**), double-immunohistochemical staining photos for α-smooth muscle actin and ERα in the neointima (**B**), and *in situ* hybridization of E4F1 mRNA in the neointima (**C** and **D**) of an abdominal aorta specimen obtained from a 38-year-old premenopausal woman with a mild degree of atherosclerosis (group C). **B:** Immunopositive cells for ERα appear brown as a result of diaminobenzidine colorimetric reaction. Immunopositive cells for α-smooth muscle actin appear blue as a result of Vector-blue colorimetric reaction. Double-immunopositive cells are confirmed. **C:** Negative control hybridized with sense oligonucleotide probes showed no detectable specific mRNA hybridization signals. Nuclear staining, appearing red, was performed by Kernechtrot. **D:** E4F1 mRNA hybridization signals, appearing blue, were detected in the marginal region of VSMCs in the neointima. Nuclear staining, appearing red, was performed by Kernechtrot. Ni, neointima; M, media. Original magnifications: ×100 (**A**); ×400 (**B–D**).

but CHX did not inhibit its expression. Therefore, these findings all indicated that E4F1 is considered one of the first established responsive genes in ERα-positive VSMCs. However, it is not known whether these half-EREs are associated with estrogenic actions or not.

Table 4. Results of Labeling Index (LI) for Target Gene (E4F1) mRNAs in VSMCs of Human Aorta

Group	*n*	Neointima	Media
Group A	3	5.6 ± 0.5	2.0 ± 0.5
Group B	3	3.2 ± 0.4 *	2.0 ± 0.4
Group C	6	24.0 ± 2.0 *	4.8 ± 1.0
Group D	6	2.4 ± 0.5 *	3.4 ± 0.7
Group E	4	6.2 ± 1.5	4.8 ± 0.7
Total	22	7.3 ± 1.8	3.4 ± 0.4

Data are the mean ± SEM. A statistical significance was evaluated among the groups using one-way analysis of variance followed by unpaired *t*-test.
* $P < 0.05$.

Therefore, it awaits further investigation for clarification to detect a strict E4F1 promoter region and then to demonstrate whether ERα is actually binding to each ERE present at upstream region of E4F1 promoter using a chromatin immunoprecipitation assay.[36,37]

Results of our study in human aorta also demonstrated that levels of E4F1 mRNA expression were significantly higher in VSMCs of neointima of premenopausal female aorta with mild atherosclerotic changes than in those of other groups. This finding therefore suggests that E4F1 is mainly expressed in dedifferentiated/proliferating VSMCs positive for ERα in neointima of premenopausal female aorta. This finding also demonstrated that the expression of E4F1 may be strongly induced by estrogens via ERα in VSMCs present at neointima of those aorta, possibly involved in inhibitory actions of VSMC proliferation by estrogens to prevent neointimal formation.[38]

SERMs are postulated to be an attractive alternative with respect to cardiovascular risk reduction, providing

that they exert cardioprotective effects like estrogens. SERMs act as ER antagonists in the breast and uterus, avoiding the harmful effects of estrogens but presumably preserving the beneficial effects of estrogens on bone, lipids, and the cardiovascular system.[39–41] In addition, it is known that TAM binds with similar affinity to both ERs, whereas RAL has a higher affinity for ERα.[42,43] Moreover, a previous report demonstrated that TAM has partial agonist activities on anti-atherogenic effects and vascular reactivity through interaction with ERα but not with ERβ in human VSMCs.[9] These all may be consistent with results of our present study. It is also postulated that estrogenic effects by SERMs are induced through AP-1 pathway.[35] However, several previous reports also documented that pretreatment of SERMs blocked the anti-atherogenic effects exerted by E_2 and that they have mixed estrogenic and anti-estrogenic effects on anti-atherogenesis in VSMCs and endothelial cells.[44–46] Both TAM and RAL are reported to inhibit the classical ERE pathway described above activated by E_2 when these cells are treated together with E_2 and SERMs,[35] which is also consistent with these above reports.[44–46] Results of quantitative RT-PCR and cell proliferation studies also demonstrated that E4F1 was induced by estrogens and suppressed the cell proliferation in ERα-positive VSMCs, but not by TAM or RAL, which may be partially consistent with results of these above reports. Therefore, SERMs may also be involved in inhibition of ERα-positive VSMC proliferation not through the above classical pathway induced by E4F1 based on results of our present investigations. These results all suggest the possible involvement of other pathways of estrogenic inhibition of VSMC proliferation. This may be also consistent with a previous report demonstrating that SERMs exert an anti-proliferative effect in VSMCs, at least in part through a p38 cascade whose activation is mediated by ERα via a non-genomic mechanism.[47] However, further investigations are required to determine how these above pathways interact with each other in estrogenic and/or anti-estrogenic effects on VSMCs, and to examine whether there are other possible pathways involved in estrogenic anti-atherogenic processes in human VSMCs *in vivo*, including an analysis of the difference between E_2 and SERMs.

In our study, estrogens demonstrated no inhibitory effects in proliferation of ERβ-positive VSMCs. In addition, results of our present study also demonstrated that the inhibitory actions of VSMC proliferation via E4F1 were not detected in these VSMCs, whereas ERβ was reported to be predominantly expressed in VSMCs.[9] Furthermore, ERβ has recently been demonstrated not only to play an essential role in the regulation of vascular function and blood pressure, but also to be associated with several mechanisms of anti-atherogenic effects.[48–50] These previous reports of *in vitro* studies all suggest that E_2 was associated with growth inhibitory actions in porcine and/or rat VSMCs predominantly through ERβ stimulation.[50,51] The signaling pathway mediating growth inhibition via ERβ has been also reported to be through reduction of p42/44 and p38 MAPK activity, and/or the cyclic AMP-adenosine pathway.[49–52] These signaling pathways may be attributable to the nongenomic action of E_2.[53,54] However, ERβ is well-known as a relatively less potent transactivator than ERα at low receptor concentrations, such as in our T/G HA-VSMC cell lines, in response to E_2.[9] This may be one of the reasons to explain the absence of an inhibitory role of estrogenic signals via ERβ on VSMC proliferation demonstrated in our present study. ERβ is also reported to predominantly increase after injury to the carotid artery of rat, and may be also consistent with promoting inhibitory actions through increment of ERβ concentrations.[55] On the other hand, previous studies on vascular injury using fully null ERα knockouts indicated that ERα is basically and predominantly important for anti-atherogenic effects of estrogen in mice, which is consistent with results of our present study.[13] However, according to these several previously published reports, it is difficult to exclude the possibility that which ER is more important for anti-atherogenesis depends on difference of species. Therefore, it still remains unclear which subtype of ER is more important for estrogenic anti-atherogenic effects in human, although our present study demonstrated the above pathway through ERα and E4F1. In addition, all previous reports have demonstrated several pathways of estrogen-induced anti-atherogenic effects *in vitro* but not *in vivo*, and therefore it remains unclear which pathway is most important for ERα-mediated anti-atherogenic effects *in vivo*. Further investigations in atherosclerotic models or in human cardiovascular system are required for clarification.

In conclusion, E4F1 is considered one of the estrogen-responsive genes involving ERα-mediated inhibition of VSMC proliferation and may play important roles in estrogen-related atheroprotection of human aorta.

Acknowledgment

We thank Naomi Kanai for technical assistance.

References

1. Stampfer MJ, Colditz GA, Willett WC, Manson JE, Rosner B, Speizer FE, Hennekens CH: Postmenopausal estrogen therapy and cardiovascular disease. N Engl J Med 1991, 325:756–762
2. Viscoli C, Brass L, Kernan W, Sarrel P, Suissa S, Horowitz R: A clinical trial of estrogen-replacement therapy after ischemic stroke. N Engl J Med 2001, 345:1243–1249
3. Rossouw JE, Anderson GL, Prentice RL, LaCroix AZ, Kooperberg C, Stefanick ML, Jackson BD, Beresford SA, Howard BV, Johnson KC, Kotchen JM, Ockere J: Writing Group for the Women's Health Initiative Investigators: Risk and benefits of estrogen plus progestin in healthy postmenopausal women. Principal results from the Women's Health Initiative randomized controlled trial. JAMA 2002, 288:321–333
4. Hulley S, Furberg C, Barrett-Connor E, Cauley J, Grady D, Haskell W, Knopp R, Lowery M, Satterfield S, Schrott H, Vittinghoff E, Hunninghake D: HERS Research Group. Noncardiovascular disease outcomes during 6.8 years of hormone therapy. HERS II. JAMA 2002, 288:58–66
5. Sullivan TR, Karas RH, Aronovitz M, Faller GT, Ziar JP, Smith JJ, O'Donnell TF, Mendelson ME: Estrogen inhibits the response-to-injury in a mouse carotid artery model. J Clin Invest 1995, 96:2482–2488
6. Hodgin JB, Krege JH, Reddick RL, Korach KS, Smithies O, Maeda N: Estrogen receptor α is a major mediator of 17β-estradiol's anti-atherogenic effects on lesion size in Apoe$^{-/-}$ mice. J Clin Invest 2001, 107:333–340
7. Kuiper GG, Enmark E, Pelto-Huikko M, Nilsson S, Gustafsson JÅ·